



DELHI TECHNOLOGICAL UNIVERSITY

(Formerly Delhi College of Engineering)

Shahbad Daulatpur, Main Bawana Road, Delhi-42

CANDIDATE'S DECLARATION

I **Subodh Bende** hereby certify that the work which is being presented in the thesis entitled **Novel Method for Finding the Interfacial Shear Stress between FRP-Concrete Interface** in partial fulfilment of the requirements for the award of the Degree of Master in Technology, submitted in the Department of **Civil Engineering**, Delhi Technological University is an authentic record of my own work carried out during the period from **August,2023** to **May,2024** under the supervision of **Dr. Shilpa Pal and Dr. Naveet Kaur**

The matter presented in the thesis has not been submitted by me for the award of any other degree of this or any other Institute.

Subodh
31/05/24
(**Subodh Bende**)

This is to certify that the student has incorporated all the corrections suggested by the examiners in the thesis and the statement made by the candidate is correct to the best of our knowledge.

Naveet Kaur

Dr. Naveet Kaur

(Co-Supervisor)

Place :Delhi

Date:

Shilpa Pal

Dr. Shilpa Pal

(Supervisor)

The viva voice of Mr. Subodh Bende has been held on

(Signature of External Examiner)



DELHI TECHNOLOGICAL UNIVERSITY

(Formerly Delhi College of Engineering)

Shahbad Daulatpur, Main Bawana Road, Delhi-42

CERTIFICATE BY THE SUPERVISOR(S)

Certified that **Subodh Bende** (2K22/STE/17) has carried out his search work presented in this thesis entitled “Novel Method for Finding the Interfacial Shear Stress Between FRP-Concrete Interface”, for the award of **Master of Technology** from Department of Civil Engineering, Delhi Technological University, Delhi, under our supervision. The thesis embodies results of original work, and studies are carried out by the student himself and the contents of the thesis do not form the basis for the award of any other degree to the candidate or to anybody else from this or any other University/Institution.

Signature

Dr. Naveet Kaur
Senior Scientist
CSIR-CRRI

Signature

Dr. Shilpa Pal
Associate Professor
Delhi Technological University

Date

Novel Method for Finding the Interfacial Shear Stress Between FRP-Concrete Interface

Subodh Bende

ABSTRACT

Fiber Reinforced Polymer (FRP) materials have gained significant attention in the construction industry due to their high strength, durability, and corrosion resistance properties. One critical aspect in the design and analysis of FRP-restrengthened structures is the evaluation of shear stress at the interface between FRP and concrete. Accurate determination of this shear stress is essential for ensuring the structural integrity and performance of FRP-strengthened elements.

Traditional methods for evaluating interfacial shear stress have limitations for accurately capturing the complex interactions between FRP and concrete. This research proposes a novel method for calculating shear stress at the FRP-concrete interface, taking into account the simplicity of the specimen, test apparatus and accuracy.

For the study, three different cylindrical specimens, of size 100 mm and height 273.2 mm were cast to calculate the interfacial shear stress between FRP and concrete. The FRP sheet was applied in an inclined plane, making an angle of 30° with the vertical face of the cylinder.

In this research, experimental investigations were conducted to gather data on the bond behavior of FRP-concrete interfaces using a UTM machine. Emphasis is focus on understanding the influence of parameters such as surface preparation, adhesive properties, and specimen size on interfacial shear stress.

The proposed method offers a comprehensive approach to assess shear stress at the FRP-concrete interface, considering the complex interactions between materials and loading conditions. By incorporating simple experimental arrangement, this research provides a valuable tool for designing and analyzing FRP-strengthened structures with improved accuracy and reliability.

Moreover, an analytical study was also performed to evaluate the effect of the FRP sheet on the flexural capacity of the beam. The FRP sheet was applied to the soffit of the beam for the study and the last study was done to numerically investigate the effect of varying thickness of FRP and Epoxy in an inclined plane of the cylindrical sample.

The experimental study revealed that the bond strength between the FRP and the concrete element was determined to be 4.67 MPa. This finding was obtained through a series of controlled tests designed to measure the adhesion between the FRP material and the concrete substrate. The measured bond strength of 4.67 MPa indicates a robust interaction between the two materials, which is critical for the effectiveness of FRP

reinforcement in structural applications. These results provide important insights for the design and implementation of FRP systems in enhancing the durability and performance of concrete structures.

The analytical investigation into the effect of the FRP sheet on the flexural capacity of the beam revealed that by applying a 4.04 mm thick FRP sheet, the flexural capacity of the beam increased by 8.60%. The 4.04 mm FRP sheet, strategically bonded to the soffit of the beam, provided additional tensile reinforcement, effectively enhancing its load-bearing capacity. The 8.60% increase in flexural capacity signifies a substantial improvement, demonstrating the effectiveness of FRP sheets in strengthening concrete beams and extending their service life.

The numerical investigation conducted to study the effect of varying thicknesses of FRP sheets and epoxy on bond stress revealed that by applying a thicker layer of epoxy on the inclined plane in a cylindrical sample significantly increases the shear capacity of the interface. By varying the thickness of the epoxy layer, the study was able to analyse its impact on the bond stress and overall shear capacity of the interface. The results indicated that a thicker epoxy layer enhances the adhesion between the FRP and concrete, thereby improving the interface's resistance to shear forces.

ACKNOWLEDGEMENTS

Completing the research thesis, "**Novel Method for Finding the Interfacial Shear Stress between FRP-Concrete Interface**," has been a journey filled with challenges, growth and invaluable support. As i reflect on this endeavour, I am deeply grateful to all those who have played a role in its realization.

First and foremost, I extend my heartfelt gratitude to my thesis supervisor, **Dr. Shilpa Pal**, whose guidance, expertise, and unwavering support have been instrumental in shaping this research. Their mentorship and encouragement have been invaluable throughout every stage of this project.

I am indebted to my co-supervisors, **Dr. Naveet Kaur & Dr. Pardeep Kumar** for their insightful feedback, constructive criticism, and scholarly guidance. Their expertise has significantly enriched the quality and depth of this thesis.

I am grateful to the my research institute, Central Road Research Institute(CRRI) for providing the necessary resources, facilities, and academic environment conducive to research. The institutional support has been vital in facilitating the completion of this study.

I would like to acknowledge the assistance and cooperation of my colleagues ,**Bimal Sharma** and helpers **Shiva, Satish & Sumit**, whose discussions, feedback, and encouragement have been invaluable throughout this journey. Their camaraderie and support have made this endeavour all the more rewarding.

Lastly, I am deeply grateful to my family and Vasudev ji for their unwavering support, patience, and understanding during this academic pursuit. Their love and encouragement have been a constant source of strength and motivation.

In conclusion, I extend my sincere appreciation to all individuals and entities who have contributed to this research thesis, directly or indirectly. Your support has been instrumental in its completion.

Thank you



31/05/24
(Subodh Bende)

TABLE OF CONTENTS

Title	Page no.
Candidates Declaration	ii
Certificate by the Supervisor's	iii
Abstract	iv
Acknowledgements	vi
List of Tables	x
List of Figures	xi
List of Symbols and Abbreviations	xiii

CHAPTER 1 INTRODUCTION

1.1	General	1
1.2	Fiber Reinforced polymer.....	2
1.3	Types of fiber reinforced polymer.....	3
1.3.1	Carbon Fiber Reinforced Polymer (CFRP).....	3
1.3.2	Glass Fiber Reinforced Polymer (GFRP)	3
1.3.3	Aramid Fiber Reinforced Polymer (AFRP)	3
1.3.4	Natural Fiber Reinforced Polymer (NFRP)	4
1.3.5	Basalt Fiber Reinforced Polymer (BFRP).....	4
1.3.6	Hybrid Fiber Reinforced Polymer (HFRP).....	4
1.4	Advantages of using FRP composites	5
1.5	Objectives of the Study	5
1.6	Organization of thesis.....	6

CHAPTER 2 LITERATURE REVIEW

2.1	Introduction	7
2.2	Different Test for calculating the shear stress between FRP-Concrete Interface.....	7
2.2.1	Single Lap Shear Test	8
2.2.2	Double Lap Shear Test.....	8
2.2.3	Simplified Double Lap Shear Test.....	9

2.2.4	Beam Test with Notch.....	10
2.2.5	Bond stress measured in strengthened RC Beam.....	11
2.3	Gap of the Study.....	11
CHAPTER 3 ANALYTICAL METHOD TO FIND FLEXURAL STRENGTH OF A RCC BEAM REINFORCED WITH FRP		
3.1	General	13
3.2	Analytical model	14
3.3	Case study for a beam with different reinforcement conditions.....	17
3.3.1	Data for analytical study of beam and FRP	17
3.4	Calculation of Flexural Capacity of Beam for different Case Study Models 18	
3.5	Curve Obtained.....	20
3.6	Discussion and Concluding remarks	21
CHAPTER 4 NOVEL EXPERIMENTAL METHOD FOR FINDING INTERFACIAL SHEAR STRESS BETWEEN FRP AND CONCRETE		
4.1	Introduction	22
4.2	Methodology	22
4.3	Mix Preparation.....	23
4.3.1	Cement:	24
4.3.2	Aggregates.....	24
4.3.3	Admixtures:.....	24
4.3.4	Water	25
4.3.5	Design Mix Calculation	25
4.4	Problems occur while casting the samples	27
4.4.1	Preparation of Molds from PVC pipe	28
4.5	Learnings while casting the samples	29
4.6	Lab Work for preparation of sample	31
4.6.1	Cylindrical Sample Preparation	32
4.6.2	Casting of Concrete Cube	37
4.7	Testing of samples.....	38
4.7.1	Testing of concrete cubes.....	39
4.7.2	Testing of cylindrical specimens.....	40
4.8	Data Obtained from UTM	41

4.8.1	41
4.8.2	41
4.9 Validation of obtained experimental results with ANSYS software.....	43
4.9.1 Input data.....	43
4.9.2 Modelling	43
4.9.3 Analysis.....	44
4.9.4 Results obtained	45
4.9.5 Obtained Result Validation	47
4.10 Concluding remarks	47
CHAPTER 5 NUMERICAL INVESTIGATION TO PERFORM PARAMETRIC STUDY FOR INTERFACIAL SHEAR STRESS BETWEEN FRP AND CONCRETE	
5.1 General	49
5.2 Problems	50
5.3 Finite-Element Analysis and Implementation	50
5.3.1 Numerical Modelling	51
5.4 Results from Analysis	53
5.4.1 Contours obtained for different thickness of FRP	55
5.4.2 Curves obtained for different thickness of FRP and Epoxy.....	56
5.5 Concluding remarks	58
CHAPTER 6 CONCLUSION AND FUTURE WORK	
6.1 Summary	59
6.2 Conclusions	60
6.3 Future Scope.....	61
REFERENCES.....	63
SCOPUS INDEX CONFERENCES.....	66
PROFILE.....	70
PLAGIARISM REPORT.....	71

List of Tables

Table 3.1	Different values of Environmental reduction factor (C_E).....	15
Table 3.2	Properties of RC Beam.....	18
Table 3.3	Properties of FRP system	19
Table 4.1	Calculated Design Mix for 1 cum of concrete	27
Table 4.2	Required Concrete contents for required volume.....	27
Table 4.3	Technical data sheet for Epoxy	34
Table 4.4	Different mechanical properties for Epoxy (Part A and Part B)	34
Table 4.5	Material properties of FRP	36
Table 4.6	Data obtained from UTM for cubical samples	41
Table 4.7	Data obtained from UTM for cylindrical samples	43
Table 4.8	Analysis data obtained from ANSYS Software	46
Table 5.1	Materials properties	51
Table 5.2	Different combination of FRP and Epoxy Thickness	52
Table 5.3	Stresses in different planes	54
Table 5.4	Maximum shear stress with respect to different thickness of Epoxy and FRP.....	55

List of Figures

Fig. 2.1	Model image for Single lap shear test with reaction frame (Kumar, 2021) ...	8
Fig. 2.2	Model image for Double lap shear test (Kumar,2021).....	9
Fig. 2.3	Simplified double shear test with loading conditions (Kumar,2021).....	10
Fig. 2.4	Beam test set up with notch at soffit of beam (Kumar,2021).....	10
Fig. 3.1	Image representing idealized simply supported beam without FRP reinforcement	19
Fig. 3.2	Image representing idealized simply supported beam reinforced with FRP20	
Fig. 3.3	Curve between different thickness of FRP and Moment carrying capacity 21	
Fig. 4.1	Flow chart of methodology.....	23
Fig. 4.2	Cylindrical Sample represent the required angle from vertical face of the cylinder.....	28
Fig. 4.3	Marking done on the PVC pipe	29
Fig. 4.4	Image showing the required plane of separation of molds after running the hexa blade.....	29
Fig. 4.5	Image showing the different orientation of molds prepared from the PVC Pipe.....	30
Fig. 4.6	Image represents the flow of concrete on the top surface of molds	30
Fig. 4.7	Placing of molds in the pit with a flat plywood supported at the inclined surface	31
Fig. 4.8	Grinding machine used for leveling of surface	32
Fig. 4.9	Grinding operation done on the inclined concrete surface	32
Fig. 4.10	Surface obtained after grinding operation	33
Fig. 4.11	Saturant-A(left one) and Saturant-B(Right one) of Epoxy.....	33
Fig. 4.12	Manual mixing of two parts of Epoxy.....	35
Fig. 4.13	Application of Epoxy to the inclined surface of Concrete for fixation of FRP sheet	35
Fig. 4.14	Image representing complete fixation of FRP sheet to concrete surface ...	36
Fig. 4.15	Complete assembly to provide lateral and longitudinal support to cylindrical specimen.....	37
Fig. 4.16	Concrete mix filled in cubical molds.....	38
Fig. 4.17	Concrete cubes taken out of curing tank for testing	39
Fig. 4.18	Placing of concrete cube sample in the UTM for testing	39
Fig. 4.19	Crushed Concrete Sample	40
Fig. 4.20	Placing of cylindrical sample in the UTM for testing	40
Fig. 4.21	Images show the slipping of two interfaces of cylindrical sample at peak level of load.....	41
Fig. 4.22	Images shows dimension of major and minor axis of inclined surface.....	42
Fig. 4.23	Calculation of peak load	42

Fig. 4.24	Images represent cylindrical sample modelled in ANSYS	44
Fig. 4.25	Image represents uniform areal load (pressure) is applied at bottom end of the sample.....	44
Fig. 4.26	Image represents Mesh properties	45
Fig. 4.27	Pressure application	45
Fig. 4.28	Image represents the variation of shear stress along the inclined plane	47
Fig. 5.1	Cylindrical Model with FRP at inclined surface	51
Fig. 5.2	(a) FE Model represent mesh size (b) Mesh properties.....	52
Fig. 5.3	Finite Element Model represents boundary conditions	53
Fig. 5.4	Geometry for obtaining plane of maximum shear stress	53
Fig. 5.5	Graph represents shear stress variation in different planes	54
Fig. 5.6	Contour showing the shear stress variation in plane 2, when $T_f=0.10$ mm and $T_e=2.0$ mm.....	55
Fig. 5.7	Contour showing the shear stress variation in plane 2,when $T_f=0.15$ mm and $T_e=2.0$ mm.....	56
Fig. 5.8	Contour showing the shear stress variation in plane 2,when $T_f=0.20$ mm and $T_e=2.0$ mm.....	56
Fig. 5.9	Curve between Shear Stress and Epoxy Thickness, for $T_f=0.10$ mm	57
Fig. 5.10	Curve between Shear Stress and Epoxy Thickness, for $T_f=0.15$ mm	57
Fig. 5.11	Curve between Shear Stress and Epoxy Thickness, for $T_f=0.20$ mm	57

List of Symbols

- A_s, A_{st} - Area of nonprestressed steel reinforcement
- A_f - Area of FRP external reinforcement
- b - width of compression face of member
- c - Distance from extreme compression fiber to the neutral axis
- C_E - Environmental reduction factor
- d - Distance from extreme compression fiber to centroid of tension reinforcement, effective depth
- d_f - Effective depth of FRP flexural reinforcement
- E_c - Modulus of Elasticity of concrete
- E_f - Tensile modulus of elasticity of FRP
- E_s - Modulus of Elasticity of steel
- f_c' - Specified compressive strength of concrete
- f_{ck} - Characteristic compressive strength of concrete
- f_{fe} - Effective stress in the FRP; stress attained at section failure
- f_{fu} - Design Ultimate Tensile Strength of Cement
- f_{fu}^* - Ultimate Tensile Strength of the FRP material
- f_s - Stress in nonprestressed steel reinforcement
- f_y - Specified yield strength of nonprestressed steel reinforcement
- I_{cr} - Moment of inertia of cracked section transformed to concrete
- k - Ratio of depth of neutral axis to reinforcement depth measured from extreme compression fiber
- M_{DL} - Dead load moment
- M_{ns} - Contribution of steel reinforcement to nominal flexural strength
- M_{nf} - Contribution of FRP reinforcement to nominal flexural strength
- M_n - Nominal Flexural Strength
- M_u - Moment of resistance
- $M_{u,lim}$ - Limiting Moment of resistance
- n - Number of plies of FRP reinforcement
- t_f - Nominal thickness of one ply of FRP reinforcement

w_f - Width of FRP reinforcing plies

x_u - Depth of Neutral Axis

$x_{u,max}$ - Limiting value of x_u

Φ - Strength reduction factor

α_1 - Multiplier on f_c' to determine intensity of an equivalent rectangular stress distribution for concrete

β_1 - Ratio of depth of equivalent rectangular stress block to depth of the neutral axis

ϵ_{bi} - Strain in concrete substrate at time of FRP installation

ϵ_{fu} - Design rupture strain of FRP reinforcement

ϵ_{fu}^* - Ultimate rupture strain of FRP reinforcement

ϵ_{fe} - Effective strain in FRP reinforcement attained at failure

ϵ_{fd} - Debonding strain of externally bonded FRP reinforcement

ϵ_c - Strain in concrete

$\epsilon_{c'}$ - Compressive strain of unconfined concrete corresponding to f_c' , may be taken as 0.002

ϵ_s - Strain in non-prestressed steel reinforcement

Ψ_f - FRP strength reduction factor

List of Abbreviations

DLST-Double lap Shear Test

FRP-Fiber Reinforced Polymer

PVC- Polyvinyl Chloride

SLST- Single lap Shear Test

CHAPTER 1

INTRODUCTION

1.1 General

In the realm of civil engineering and infrastructure management, the concept of retrofitting stands as a crucial endeavour aimed at fortifying existing structures against a myriad of challenges, including aging, environmental hazards, and evolving performance requirements. Retrofitting embodies a proactive approach to enhancing structural resilience, prolonging service life and ensuring the safety and functionality of built environments for current and future generations.

Strengthening existing reinforced concrete (RC) structures is a common necessity for a multitude of reasons. Such requirements may arise from structural deficiencies stemming from faulty design, minor construction errors, or deterioration caused by natural phenomena like floods or corrosion of reinforcing bars (rebars). As societal needs evolve and performance standards increase, the demand for effective retrofitting techniques has surged. Moreover, in an era marked by sustainability and economic prudence, there is a growing preference for extensive rehabilitation over outright demolition of structures that have fulfilled their original purpose. The imperative to retrofit existing structures is multifaceted.

Some of the techniques commonly adopted for the strengthening and stiffening of RC structural element are (i) Provision of additional reinforcement with a cast-in-situ or cover of sprayed concrete(Heiza et al.,(2014)) , (ii) Strengthening by external pre-stressing Chen and Gu (2005), (iii) Impregnating the concrete with a polymer like epoxy resin under high pressure(Kanakubo et al. (2005)), (iv) Externally bolting steel plates on RC beams weak in shear or flexure and (v) Strengthening by externally bonded plates (Barnes et al. (2001); Blanksvärd et al. (2009); Hemaanitha and Kothandaraman (2014); Hussain et al. (1995); Jumaat and Alam (2009); Teng et al. (2002); Ye (2001))

1.2 Fiber Reinforced polymer

Fiber Reinforced Polymer (FRP), also known as fiber-reinforced plastic, is a composite material made up of a polymer matrix reinforced with fibers. These fibers are usually made of materials such as carbon, glass, or aramid. FRP offers a combination of high strength, low weight, corrosion resistance, and design flexibility, making it a popular choice in various industries including aerospace, automotive, construction, marine, and sports equipment. Carbon Fiber Reinforced Polymer (CFRP) materials are increasingly being used in civil engineering, especially for reinforcing and strengthening reinforced concrete (RC) structures. These materials come in different forms, including pre-cured systems like strips or bars, wet lay-up systems such as sheets or mats, and prepreg systems. The growing interest in CFRP materials is due to their many advantages compared to traditional materials, such as their exceptional strength, lightweight properties, ease of application, and resistance to corrosion(Arruda et al. (2016)).

One of the key components of FRP is the polymer matrix, which can be epoxy, polyester, vinyl ester, or other thermosetting or thermoplastic resins. These matrices provide structural integrity and hold the fibers together, while the fibers impart strength and stiffness to the composite.

The predominant method for applying pre-cured CFRPs onto concrete involves the use of externally bonded reinforcement (EBR) technique. In this approach, CFRP strips or sheets are affixed externally, typically using epoxy, onto the surface of the structural member requiring reinforcement. A newer method, known as near surface mounted (NSM), has emerged where CFRP reinforcement (strips or bars) is inserted and bonded within saw-cut slits made in the concrete cover. This NSM technique has been effectively implemented in recent times. (Arruda et al. (2016)). Overall, Fiber Reinforced Polymers offer a compelling combination of strength, lightweight, corrosion resistance, design flexibility, and environmental sustainability, making them a versatile choice for a wide range of applications across various industries.

1.3 Types of fiber reinforced polymer

Fiber Reinforced Polymers (FRPs) encompass a variety of composite materials where fibers are embedded within a polymer matrix to enhance mechanical properties. These fibers can be made of various materials, each offering unique characteristics suitable for different applications. Here are some common types of fiber reinforced polymers

1.3.1 Carbon Fiber Reinforced Polymer (CFRP)

- **Fibers** Made from carbon atoms bonded together in crystals with a diameter of about 5-10 micrometres.
- **Properties** Exceptional strength-to-weight ratio, high stiffness, low thermal expansion, and excellent fatigue resistance.
- **Applications** Aerospace, automotive, sporting goods, civil engineering (e.g., reinforcement of structures), and high-performance equipment.

1.3.2 Glass Fiber Reinforced Polymer (GFRP)

- **Fibers** Composed of fine glass fibers, typically made from silica-based materials.
- **Properties** Relatively low cost, good tensile strength, flexibility, and resistance to environmental factors.
- **Applications** Construction (reinforcing structures, pipes, tanks), automotive parts, marine components, electrical insulators, and consumer goods.

1.3.3 Aramid Fiber Reinforced Polymer (AFRP)

- **Fibers** Aramid fibers, such as Kevlar, are long-chain synthetic polymers with high strength and heat resistance.
- **Properties** Exceptional strength, resistance to impact, good heat resistance, and low weight.

- **Applications** Body armor, aerospace components, sporting goods (e.g., racing helmets), and high-performance equipment requiring durability.

1.3.4 Natural Fiber Reinforced Polymer (NFRP)

- **Fibers** Derived from natural sources such as plant fibers (e.g., bamboo, hemp) or animal fibers (e.g., wool, silk).
- **Properties** Biodegradable, renewable, relatively low cost, and good thermal insulation properties.
- **Applications** Automotive interiors, construction materials, packaging, and consumer goods aiming for sustainability.

1.3.5 Basalt Fiber Reinforced Polymer (BFRP)

- **Fibers** Made from basalt rock melted at high temperatures and drawn into fibers.
- **Properties** High tensile strength, resistance to chemicals and corrosion, and excellent thermal stability.
- **Applications** Construction (reinforcing concrete), marine structures, automotive parts, and thermal insulation.

1.3.6 Hybrid Fiber Reinforced Polymer (HFRP)

- **Fibers** Combination of different types of fibers (e.g., carbon, glass, aramid) within the same polymer matrix.
- **Properties** Tailored to specific requirements by combining the advantages of different fiber types.
- **Applications** Structural components where a balance of properties such as strength, weight, and cost-effectiveness is essential.

These types of fiber reinforced polymers offer a wide range of options for engineers and designers to select materials best suited for their specific applications, considering factors such as mechanical properties, cost, environmental impact, and sustainability requirements.

1.4 Advantages of using FRP composites

Fiber Reinforced Polymer (FRP) composites offer numerous advantages across diverse industries and applications. Their exceptional strength-to-weight ratios make them notably lighter than traditional materials like steel or concrete, while still upholding comparable strength and structural integrity. This characteristic significantly reduces transportation costs, facilitates easier handling during installation, and enables the design of more efficient and sustainable structures. Additionally, FRP composites boast excellent corrosion resistance, making them well-suited for environments prone to chemical exposure, moisture, or harsh weather conditions. Their non-conductive properties also render them suitable for applications requiring electrical insulation, thus expanding their utility in both infrastructure and industrial settings. Moreover, FRP composites provide design flexibility, allowing for the creation of complex shapes and forms that may be challenging or costly with conventional materials. They are inherently durable and boast long service lives, necessitating minimal maintenance over time and reducing life-cycle costs. Furthermore, FRP composites serve as environmentally friendly alternatives due to their recyclability and lower embodied energy compared to traditional materials. This contributes to sustainability efforts and aligns with green building practices. In summary, the advantages of FRP composites encompass lightweight construction, corrosion resistance, design flexibility, durability, and environmental sustainability, driving their increasing adoption across a wide array of industries, including aerospace, automotive, construction, marine, and infrastructure.

1.5 Objectives of the Study

This research aims to provide a comprehensive and accurate assessment of the shear stress occurring at the interface between the FRP material and the concrete substrate. By utilizing advanced experimental and computational methodologies, this novel approach seeks to overcome existing limitations and challenges in measuring interfacial shear stress.

The primary objective of the research is

- To study the Existing Method for finding the interfacial shear stress between FRP-Concrete Interface.
- To propose a Novel method for finding the interfacial shear stress between FRP-Concrete interface.

1.6 Organization of thesis

Chapter 1 gives a concise explanation of fiber-reinforced polymer and outlines the goals of the research as well as the objective of the study.

Chapter 2 provides a comprehensive literature review and gap of the study

Chapter 3 describes the detail information about the analytical method used for calculating the flexural strength of a beam reinforced with FRP

Chapter 4 presents the results of the experimental work and discussions of the outcomes for finding the shear stress in an inclined plane

Chapter 5 presents the result of the numerical works done for finding the interfacial shear stress in an inclined plane of the cylinder

CHAPTER 2

LITERATURE REVIEW

2.1 Introduction

Strengthening existing reinforced concrete (RC) structures is frequently necessary for a variety of reasons. Such needs may arise from design flaws, minor construction errors, or damage resulting from natural occurrences like flooding or rebar corrosion. The importance of strengthening techniques has grown due to the rising trend of enhancing existing concrete structures to meet increased performance requirements. Additionally, extensive rehabilitation efforts are often favoured over demolishing structures that have fulfilled their initial intended purpose, driven by cost-benefit considerations. On the other hand, FRP materials have gained widespread recognition for their high strength-to-weight ratio, corrosion resistance, and ease of installation, making them an attractive choice for structural strengthening and rehabilitation applications. Bonding FRP sheets or fabrics to concrete surfaces is a common practice to enhance structural capacity, improve flexural behaviour, and mitigate damage in reinforced concrete members. However, the effectiveness of FRP-concrete bonding is influenced by several factors including surface preparation, adhesive properties, FRP thickness and loading conditions etc.

2.2 Different Test for calculating the shear stress between FRP-Concrete Interface

The interface between Fiber-Reinforced Polymer (FRP) and concrete plays a crucial role in determining the overall performance and durability of FRP-reinforced concrete structures. Shear stress at this interface is a critical parameter influencing the bond strength and structural integrity. Various tests have been developed to accurately assess the shear stress between FRP and concrete interfaces, each offering unique advantages and insights. This theory explores different test methods used for calculating shear stress at the FRP-concrete interface and discusses their applicability, advantages, and limitations

2.2.1 Single Lap Shear Test

The Single-lap shear test (SLS), serves as a common method for assessing the shear stress between Fiber Reinforced Polymer (FRP) and concrete during intermediate crack debonding (ICD).

Bizindavyi and Neale (1999) and Bilotta et al. (2009) delved into SLS testing methodology. In this test configuration, FRP plates were affixed to the upper surface of concrete blocks, with the specimen secured by reaction and positioning frames to prevent uplift as shown in Fig. 2.1. Following this setup, a debonding load was applied to the plate end, inducing shear deformations. However, it's essential to note that in practical scenarios, the FRP-concrete interface experiences a combination of shear and bending forces

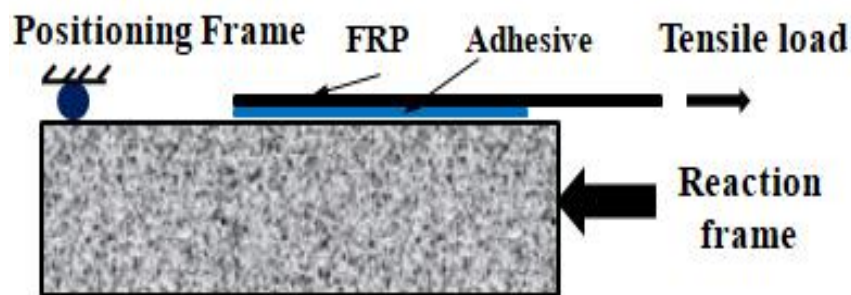


Fig. 2.1 Model image for Single lap shear test with reaction frame (Kumar, 2021)

In the test setup and loading application, it was assumed that shear stress was uniformly distributed along the width of the bond, and axial load was also applied uniformly. Contact between the specimen and the FRP-concrete interface was limited to the surface only. As a result, this single lap shear test bears resemblance to the IC debonding mechanism.

2.2.2 Double Lap Shear Test

Nakaba et al. (2001) and Camli and Binici (2007) investigated that in the double-lap shear test (DLST), FRP plates were symmetrically affixed to both sides of the prism. Subsequently, the ends of the FRP plates underwent tensile forces, resulting in the initiation of intermediate cracks at the FRP-concrete interface. In this test configuration, two equal-sized concrete prisms were prepared. FRP plates were

bonded to two opposite faces of each concrete prism, with one side of the FRP wrap applied to one side of the cube, ensuring that only one block contributed to debonding as shown in Fig. 2.2. The reaction between the concrete blocks was induced either by applying load through hydraulic jacks positioned between the blocks or by pulling steel bars.

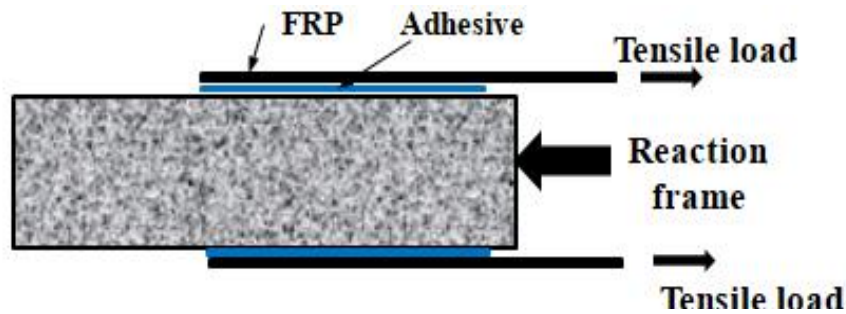


Fig. 2.2 Model image for Double lap shear test (Kumar,2021)

2.2.3 Simplified Double Lap Shear Test

The author **Larralde *et al.* (2001)** introduced a simplified approach for conducting the double-lap shear test (DLST). This method involved preparing a specimen using three cement mortar cubes, each measuring 50 mm. The mixing proportions for the cement mortar cubes were 1.0, 3.0, and 0.5 by mass of Portland cement, fine aggregate, and water, respectively. The cubes were bonded together using the tested FRP composites. The middle cube was subjected to a uniformly distributed force on its upper surface, while the other two cubes were uniformly supported on their entire bottom surface, as shown in Figure 2.3. The experimental setup was designed primarily to apply shear stresses on the interfaces between the cubes.

The study also investigated the influence of high temperature, freezing/thawing cycles, and cycles of saturation in a sulphate solution on the shear stress. Results indicated that comparing results between various cases in pairs yielded significance levels below 90%, except for paired cases involving the effects of high temperature and salt solution cycles, which exhibited significance levels greater than 95%. The study concluded that despite its variability and departure from rigorously representing actual conditions, the proposed method was straightforward to prepare

and implement. However, it emphasized the need for further research to refine and develop a more accurate and simplified testing method

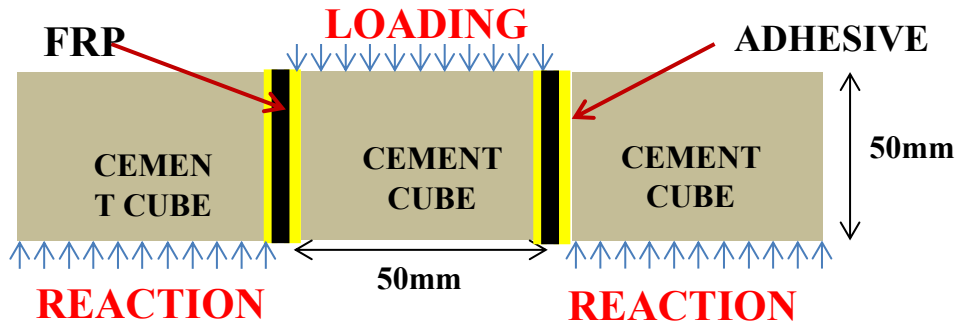


Fig. 2.3 Simplified double shear test with loading conditions (Kumar,2021)

2.2.4 Beam Test with Notch

Guo *et al.* (2005) and López-González *et al.* (2012) investigated that the stress at the interface obtained from the beam test may mimic the behaviour of the strengthened members in actual conditions. A notch was introduced at the midpoint of the beam to delineate the failure mode region prior to testing (Fig. 2.4). This testing method mirrors real-world strengthening systems because it simulates the combined

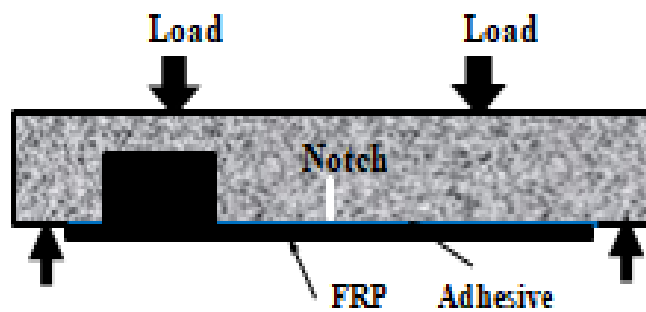


Fig. 2.4 Beam test set up with notch at soffit of beam (Kumar,2021)

effects of shear and bending at the FRP-concrete interface, as observed in practical applications. Several recent studies had investigated the bond behaviour in beam shear tests, and select findings from these studies are summarized here.

2.2.5 Bond stress measured in strengthened RC Beam

According to Ceroni et al. (2016) ;Ceroni, F., (2017) and Chen et al. (2019) the shear stress or bond stress (τ_{exp}) refers to the stress acting at the interface between the concrete and adhesive along the length of the FRP composites. This study aims to ascertain the bond or shear stress between the positions of two neighboring strain gauges. In this investigation, an equation was derived based on the principles of force equilibrium and linear elasticity, of CFRP laminate or strand sheets. The equation is as follows

$$\tau_{\text{exp}} = \frac{\varepsilon_f(x_i) - \varepsilon_f(x_{i-1})}{(x_i - x_{i-1})} \cdot E_f \cdot t_f \quad (2.1)$$

where, $x_i - x_{i-1}$ (mm) are the location of any two adjacent gauges, measured from the reference point, E_f is the FRP tensile modulus (MPa), $\varepsilon_f(x_i) - \varepsilon_f(x_{i-1})$ are strains at locations x_i & x_{i-1} , respectively, t_f is the actual thickness of the CFRP/AFRP strand sheet/laminate (mm).

2.3 Gap of the Study

The research gap in this study lies in the limited understanding of the bond behavior between FRP and concrete interfaces under various loading and parametric conditions. While existing literature provides valuable insights into the limited static behavior of these interfaces, there is a notable lack of comprehensive research focusing on dynamic loading scenarios, such as fatigue, impact, or seismic events. Additionally, there is a need for systematic investigations into the influence of surface preparation techniques, long-term performance and durability, and the development of standardized testing methods and guidelines. Addressing these gaps is crucial for accurately predicting the behavior and performance of FRP-concrete strengthening systems in real-world applications, thereby enhancing their reliability and sustainability.

Beside the above research gap, the preparation of sample used for finding the interfacial shear stress is find to be cumbersome in nature. Prestressing of reinforcement, anchorage at proper location, Grooving of Concrete is found to be

difficult process to be done on hardened concrete surface. This gap results in rendering the study less feasible and indirectly increases the cost of evaluation. Moreover, it leads to greater time consumption.

Another consideration is the method of applying the load. The equipment used for loading the samples such as hydraulic jacks, skin laminators, and vacuum infusers—is quite expensive and requires skilled engineers to operate. Consequently, accurately loading samples to measure bond stress becomes a labor-intensive task..

CHAPTER 3

ANALYTICAL METHOD TO FIND FLEXURAL STRENGTH OF A RCC BEAM REINFORCED WITH FRP

3.1 General

The retrofitting, restrengthening, and restoration of reinforced concrete frame (RCF) structures during their lifespan is a predominant challenge encountered by structural engineers globally. These structures, while in operation, might exhibit deficiencies stemming from various causes, including construction or design inaccuracies, amplified applied loads, degradation due to aging and/or environmental factors, and damage from impacts and/or corrosion (Aidoo et al. (2006); Bonacci et al. (2000); Neale, K.W., (2000)). Throughout history, improved pre-existing structures to withstand elevated design loads, rectifying strength degradation, enhancing structural effectiveness, or ductility have been achieved using different methods. These methods include some conventional techniques like applying external post tensioning, bonded steel plates, applying steel or concrete jackets (ACI 440.2R (2017)). Enhancing the resilience of reinforced concrete frame (RCF) structures externally, such as beams, columns, slabs & foundation using Fiber Reinforced Polymer (FRP) composites requires a strong adhesive bond between the composites of FRP and the concrete surface, typically achieved with epoxy resin in wet lay-up application. The layer used for adhesion plays an important role in transferring stress between the FRP and the concrete. However, an early debonding is found to be significant challenge for External Bonding Reinforcement (EBR) system (Malek et al. (1998); Sebastian, W.M. (2001)). Carbon fiber reinforced polymer (CFRP) materials are increasingly being utilized in civil engineering, especially for strengthening concrete structures. These materials are available in different configurations, including pre-cured options like strips or bars, wet lay-up systems such as mats or sheets, and prepreg systems. The growing popularity of CFRP materials can be attributed to their numerous advantages compared to traditional materials, including high strength, lightweight properties, ease of application, and resistance to corrosion (Keller, T., (2002)). The bonding

characteristics between FRP rebars and concrete layer plays an important behaviour in the local-scale load transfer mechanism and can greatly impact the mechanical behaviour of the entire FRP-reinforced concrete structures. Multiple factors influence bond behaviour, encompassing concrete compressive strength, FRP reinforcement stiffness, adhesion level between surface layer and rebar core, polymer matrix type, and fiber/matrix interface properties. These bond attributes are particularly crucial for the structures, especially regarding in-service deformations like deflections and concrete cover cracking occurrences (Rolland et al. (2020)).

FRP is a heterogeneous material made up of a polymer matrix reinforced with fibers, which generally include carbon, epoxy or aramid fibers. FRP, which stands for Fiber-Reinforced Polymer, is known for its high strength-to-weight ratio and is utilized in various engineering applications across multiple industries. These industries include aerospace, automotive, construction, and marine, among others (Fiber-Reinforced Polymer) materials are also used to enhance the moment (flexural) capacity of beams in structural engineering. This application involves externally bonding or internally embedding FRP materials to reinforce concrete or steel beams, thereby increasing their load-carrying capacity and improving their resistance to bending can enhance the flexural capacity of the beam in many ways namely through (i)Externally Bonding (ii) Near Surface Mounted (iii)Wrap Around (iv)Prestressing etc

3.2 Analytical model

For evaluate the impact of FRP sheets on the flexural capacity of the beam, a referral code is selected. The analytical code was developed by the ACI 440.2R.2017. The following are a list of equations used to calculate flexural capacity of beam, when FRP is employed at the soffit.

$$f_{fu} = C_E f_{fu}^* \quad (3.1)$$

Based on the design tensile strength, design tensile strain is calculated as per the following equation

$$\epsilon_{fu} = C_E \epsilon_{fu}^* \quad (3.2)$$

where f_{fu}^* , ϵ_{fu}^* denote design ultimate tensile strength and rupture strain of the FRP material respectively, as reported in the data sheet, psi (MPa)

C_E denotes environmental reduction factor obtained from table 9.4 of ACI 440.2R.2017

Table 3.1 Different values of Environmental reduction factor (C_E)

Exposure Condition	Fiber type	Environmental reduction factor (C_E)
Interior exposure	Aramid	0.85
	Glass	0.75
	Carbon	0.95
Exterior Exposure	Aramid	0.75
	Glass	0.65
	Carbon	0.85
Aggressive Environment	Aramid	0.70
	Glass	0.50
	Carbon	0.85

$$\beta_1 = 1.05 - 0.05(f_c' / 1000) \quad (3.3)$$

β_1 is obtained using the equation given in Section 10.2.7.3 from ACI 318-14

$$E_c = 4700\sqrt{f_c'} \quad (3.4)$$

Area of the FRP composites

$$A_f = n t_f w_f \quad (3.5)$$

$$\varepsilon_{bi} = \frac{M_{DL}(d_f - kd)}{I_{cr} E_c} \quad (3.6)$$

$$\varepsilon_{fd} = 0.41 \sqrt{\frac{f'_c}{nE_f t_f}} \leq 0.9\varepsilon_{fu} \quad (3.7)$$

Where, ε_{fd} and ε_{bi} denotes strain of externally bonded FRP bar and existing strain on the bottom of beam, respectively.

Assume approximate value of neutral axis, given by $c=0.20d$. After iterative procedure of equilibrium, the final value of c is obtained

$$\varepsilon_{fe} = 0.003 \left(\frac{d_f - c}{c} \right) - \varepsilon_{bi} \leq \varepsilon_{fd} \quad (3.8)$$

$$\varepsilon_c = \left(\varepsilon_{fe} + \varepsilon_{bi} \right) \left(\frac{c}{d_f - c} \right) \quad (3.9)$$

Where, ε_c , ε_{fe} is the strain in the concrete at failure and in the FRP reinforcement respectively.

$$\varepsilon_s = \left(\varepsilon_{fe} + \varepsilon_{bi} \right) \left(\frac{d - c}{d_f - c} \right) \quad (3.10)$$

ε_s is the strain in the existing tensile steel

$$f_s = E_s \varepsilon_s \leq f_y \quad (3.11)$$

$$f_{fe} = E_f \varepsilon_{fe} \quad (3.12)$$

Eqn.(3.11 & 3.12) are used for calculating stress in reinforcing steel (f_s) & FRP (f_{fe})

Different concrete stress block factors, obtained using ACI 318 are as follows

$$\beta_1 = \frac{4\varepsilon'_c - \varepsilon_c}{6\varepsilon'_c - 2\varepsilon_c} \quad (3.13)$$

$$\alpha_1 = \frac{3\varepsilon'_c \varepsilon_c - \varepsilon_c^2}{3\beta_1 \varepsilon_c^2} \quad (3.14)$$

Where ϵ_c' is strain at the stress level of f_c' and derived as

$$\epsilon_c' = \frac{1.7f_c'}{E_c} \quad (3.15)$$

$$c = \frac{A_s f_s' + A_f f_{fe}}{\alpha_1 f_c' \beta_1 b} \quad (3.16)$$

Where A_s is the area of steel reinforcement. This calculated value of c is used for verifying the value of neutral axis obtained earlier.

$$M_{ns} = A_s f_s' \left(d - \frac{\beta_1 c}{2} \right) \quad (3.17)$$

M_{ns} is the moment contributed from steel

$$M_{nf} = A_f f_{fe} \left(d_f - \frac{\beta_1 c}{2} \right) \quad (3.18)$$

M_{nf} is the moment contributed from FRP

$$\phi M_n = \phi [M_{ns} + \psi_f M_{nf}] \quad (3.19)$$

Where, ϕM_n denotes moment carrying capacity of the section, ψ_f is the reduction factor. This reduction factor (ψ_f) is calculated by using the reliability analysis

3.3 Case study for a beam with different reinforcement conditions

An analytical study is being conducted for the comparative analysis of beams with respect to their flexural strength, for two cases, namely

1. Flexural Capacity of beam without FRP reinforcement
2. Flexural Capacity of beam with FRP reinforcement

3.3.1 Data for analytical study of beam and FRP

The data for beam and FRP properties are shown in Table 3.2 and Table 3.3 respectively. The data for a beam and FRP arrangement is taken from a ACI CODE (440.2R-2017). The beam is reinforced along with two layer of FRP at soffit.

Table 3.2 Properties of RC Beam

Parameters	Values
Length of Beam, L	7.32 m
Width of beam, W	305 mm
Effective depth, d	546 mm
Overall depth, H	609.6 mm
Specified compressive strength of concrete, f_c'	34.5 N/mm ²
Specified yield strength of Reinforced bars, f_y	414 N/mm ²
Diameter(ϕ)	28.6 mm (3 in no.)
Dead load, w_{DL}	14.6 N/mm
Live load, w_{LL}	26.3 N/mm
Dead-load moment, M_{DL}	98 kN-m
Live-load moment, M_{LL}	176 kN-m

3.4 Calculation of Flexural Capacity of Beam for different Case Study Models

Case 1: Flexural Capacity of beam without FRP reinforcement

The beam used for the analysis has a length of 7.32 meters and a cross-section measuring 305×609.6 mm, as depicted in Figure 3.1. To determine the factored moment of the beam, calculations were performed in accordance with IS CODE 456-2000, which provides guidelines for the design and construction of reinforced concrete structures. This code ensures that the beam design adheres to standardized safety and performance criteria. The specific numerical values of the properties of the reinforced concrete (RC) beam, which are essential for calculating the flexural strength of the section, are detailed in Table 3.2.

Table 3.3 Properties of FRP system

Parameters	Values
Ultimate tensile strength, f_{fu}^*	621.00 N/mm ²
Rupture strain, ϵ_{fu}^*	0.0150 mm/mm
Modulus of Elasticity, E_f	3,70,000 N/mm ²

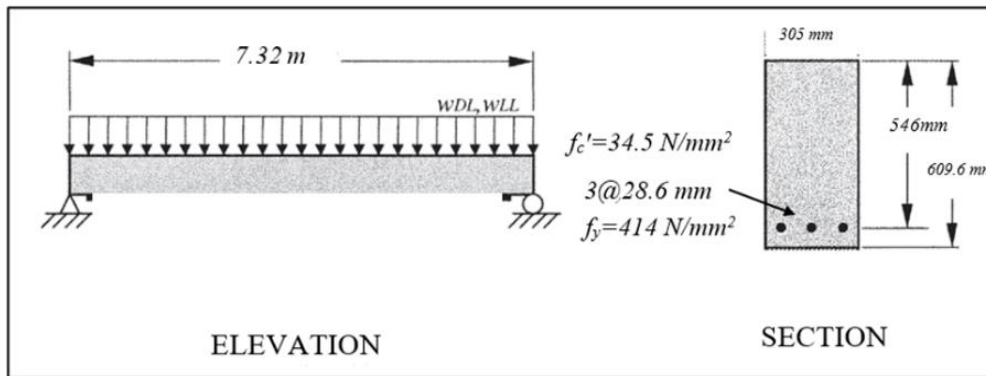


Fig. 3.1 Image representing idealized simply supported beam without FRP reinforcement

Using the tabular values (Table 3.2 and Table 3.3) and the formulas provided in IS CODE 456-2000, limiting moment for a beam has been calculated.

Note - Notations have their meanings as per IS code.

From Annexure G of IS 456-2000

$$x_u/d = (0.87f_y A_{st}) / (0.36f_{ck} b d) \quad (3.20)$$

$$M_u = 0.87f_y A_{st} d (1 - A_{st} f_y / f_{ck} b d) \quad (3.21)$$

$$M_{u,lim} = 0.36x_{u,max}/d (1 - 0.42x_{u,max}/d) b d^2 f_{ck} \quad (3.21)$$

After calculations, limiting moment come out to be **432.782 kN-m**

Case 02 - Flexural Capacity of beam using FRP as Reinforcement at soffit of beam

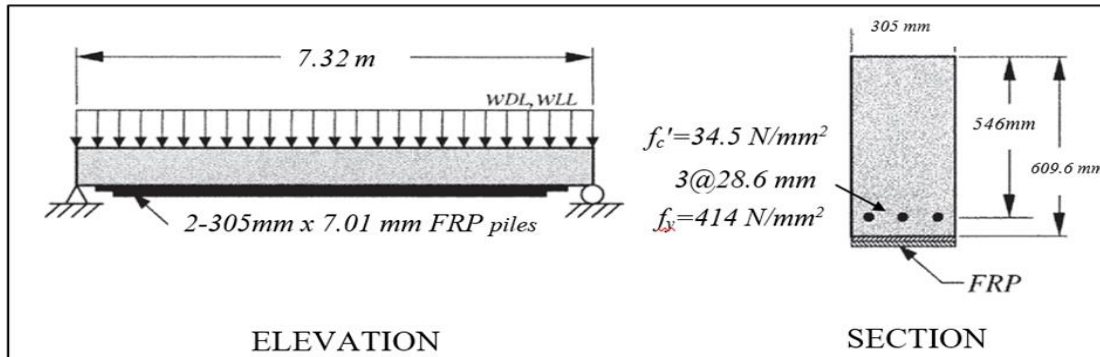


Fig. 3.2 Image representing idealized simply supported beam reinforced with FRP

The beam has a length of 7.32 m and cross-section of 305× 609.6 mm. There are two layers of FRP ply, used in the soffit of the beam. Other related important physical properties of the beam are listed in Table 3.2. Three different pairs of thickness of FRP's are employed in the system for calculate the flexural capacity of the beam. By using Eqn. (3.1-3.16) of the analytical model, the approximate value of neutral axis, c is calculated ($c=0.20d$). After iterative procedure of equilibrium, the final value of c is obtained.

Refer Table 3.3, for FRP system properties. The flexural capacity of beam calculated (using Eqn. 3.17-3.19) is shown below with the help of curve.

3.5 Curve Obtained

A pair of FRP sheets with varying thicknesses of 2.04 mm, 3.04 mm, and 4.04 mm are applied to the soffit of the beam. These variations in thickness are used to analyse how the FRP reinforcement influences the beam's moment-carrying capacity. By systematically varying the thickness of the FRP sheets, the study aims to determine the optimal thickness for enhancing the structural performance of the beam. The resulting variation in the moment-carrying capacity of the beam, as influenced by different FRP thicknesses, is illustrated in the curve as shown in Fig 3.3

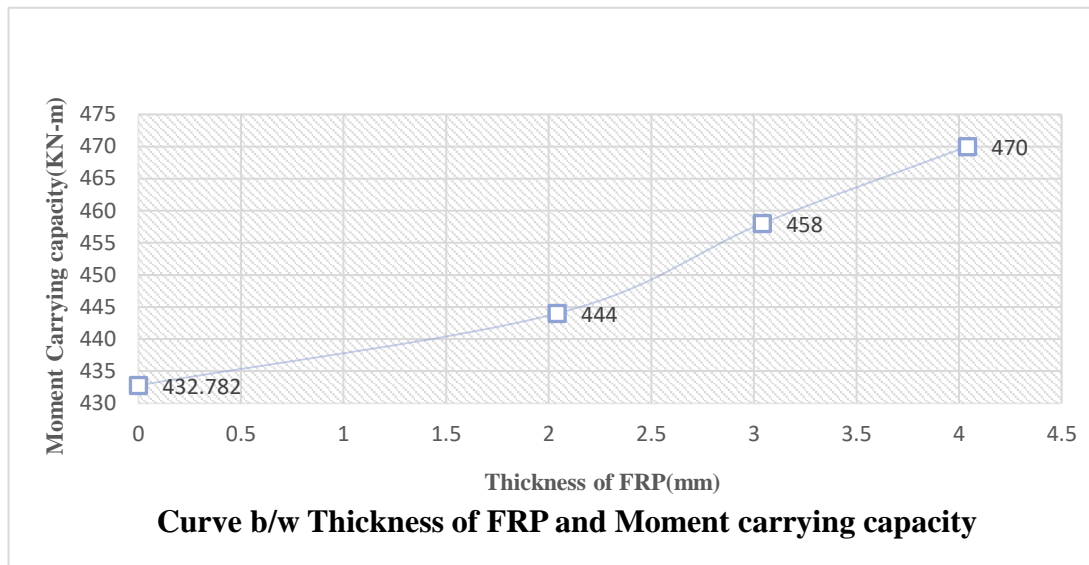


Fig. 3.3 Curve between different thickness of FRP and Moment carrying capacity

3.6 Discussion and Concluding remarks

As the thickness of the FRP sheet increases, the section modulus of the beam section correspondingly increases, resulting in greater resistance to bending and an augmented flexural capacity. This relationship stems from the fact that the section modulus of a beam section is directly influenced by the thickness of the material. Moreover, thicker FRP layers provide increased stiffness to the beam, reducing deflections under applied loads. This improved stiffness contributes to an increase in flexural capacity as the beam is better able to resist bending without excessive deformation

Proper understanding of how the thickness of FRP affects the flexural capacity allows engineers to optimize the design of FRP-reinforced concrete beams. By determining the optimal thickness for a given application, engineers ensure that the beam meets structural requirements while minimizing material usage and cost. Additionally, the study of FRP thickness contributes to the design of specific codes and standards for FRP-reinforced structures. The study shows that FRP thickness plays a vital role in enhancing the flexural capacity of beams, although its effect is non-linear in nature. It is observed that applying an FRP sheet of 4.04 mm thickness, the flexural capacity of the beam improves by 8.60%

CHAPTER 4

NOVEL EXPERIMENTAL METHODS FOR FINDING INTERFACIAL SHEAR STRESS BETWEEN FRP & CONCRETE

4.1 Introduction

Understanding interfacial shear stress holds significant importance across various disciplines, including engineering and materials science, where interfaces profoundly influence the behaviour and performance of systems. Interfaces, often serving as the boundary between distinct materials or phases. Consequently, there exists a critical need for precise and reliable experimental methodologies to predict and calculate these interactions effectively.

In this study, a novel experimental method is being approached to calculate interfacial shear stress with heightened accuracy. Meticulous experimental design and analysis aims to furnish researchers and practitioners with a robust framework for characterizing interfacial shear stress across diverse systems and applications.

This study focuses on experimental methodology, delineates the experimental setup, outlines the procedures for sample preparation and its analysis. In this study, a cylindrical specimen with a total length of 273 mm and a diameter of 100 mm was cast. A plane inclined at 30° from the vertical face of the cylinder was chosen for analysis. By shedding light on interfacial shear stress, this work sets the stage for detailed study of interfacial phenomena, thereby facilitating innovation and progress in different methods of retrofitting.

4.2 Methodology

To determine the interfacial shear stress between Fiber Reinforced Polymer (FRP) and concrete, a structured research methodology is essential. Here is a comprehensive outline of the research methodology

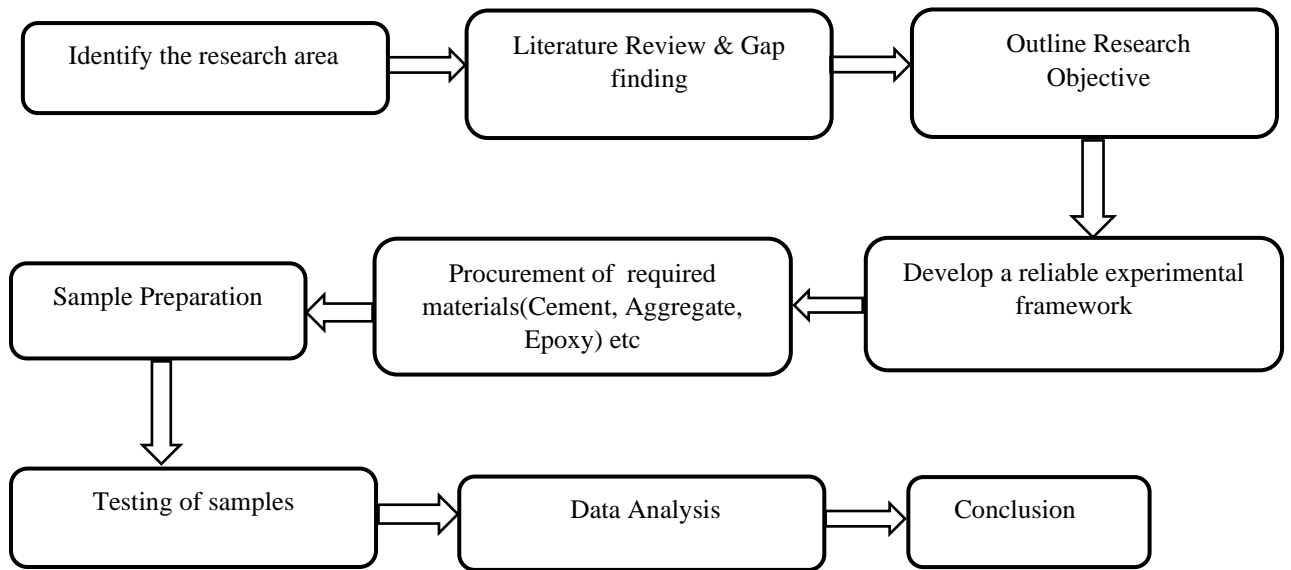


Fig. 4.1 Flow chart of methodology

The methodology for this research consists of several key steps. The first step was to identify the research area by gaining a proper understanding of the work done so far and identifying existing gaps. Next, the objectives were defined, and based on these objectives, the required experimental framework was chosen. Essential materials such as cement, sand, coarse and fine aggregate, water, FRP sheets, and epoxy (Part A and Part B) were then procured. After procuring the materials, samples were cast using molds, which were subsequently prepared for testing. A Universal Testing Machine (UTM) was used to apply compressive force during the testing of the sample, which will ultimately help to determine the bond stress at the FRP-Concrete interface. Detailed analysis of the results was then carried out using Excel software

4.3 Mix Preparation

To conduct the study, a design mix of Grade M50 was prepared for the casting of cylindrical samples and cubes. Detailed information about the process involving preparation of design mix has been discussed below. To calculate the design mix ratio, IS Code 10262-2019 (*Concrete Mix Proportioning-Guidelines*) has been used. A design mix, in the context of concrete construction, refers to a specific

combination of ingredients and proportions formulated to achieve the desired properties and performance characteristics of concrete for a particular application. Unlike nominal mixes, which use predetermined ratios based on volume, design mixes are tailored to meet specific requirements such as strength, workability, durability, and environmental conditions. The ingredients used to prepare the M50 design mix concrete are as follows

4.3.1 Cement:

For the design mix, Ordinary Portland Cement (43 Grade) had been used.

4.3.2 Aggregates

- **Coarse Aggregate :** Clean, well-graded aggregates with sizes typically ranging from 10mm to 20mm was being opted.
- **Fine Aggregate:** Clean, natural sand having a size of less than 4.75 mm, free from deleterious materials had been selected and used.

4.3.3 Admixtures:

Optional admixtures are being used to modify the properties of the concrete mix, specifically for reduction of water content is being used. For the preparation of samples, Super Plasticizer have been used. Details of which is given below.

Product Name - CEMWET SP-3000(PCE-2)

Specific Gravity - 1.10 ± 0.020

Colour - Light Yellow

Chloride Content - NIL to BS 5075, to IS 456-2000

Air Entertainment - Maximum 1.5% of Control as per IS 9103-99

Water Reduction - More than 38%

Shelf life - 2 Years

4.3.4 Water

Clean water suitable for drinking and mixing with a pH value near to 7 has been used to form a workable paste.

4.3.5 Design Mix Calculation

For the calculation of design mix(M₅₀), IS 10262-2019(*Concrete Mix Proportioning-Guidelines*) has been used. The following steps are being followed to obtain the final mix ratio.

- Target Mean Strength $f'_{ck} = f_{ck} + 1.65 S$ (From Table 2)
 $= 50 + 1.65 * 5$
 $= 58.25 \text{ N/mm}^2$
- Water-Cement ratio, $= 0.335$ (From Fig 1, Curve 2)
- Maximum water content = 186 kg (From Table 4)
- Maximum size of aggregate = 20 mm
- Ratio of Fine aggregate & Total aggregate = 0.585 (From Table 5)
- Sand Confirming zone = III
- Volume of Sand content = 0.415 m³
- Required slump value = 50 mm
- Water content = 186 kg (From Table 4)
- Actual water content = 158.10 kg (Clause 5.3)
- Cement content = 471.94 kg

Mix Calculations for 1 cum of concrete are given below:-

Required data

Specific gravity of cement(G_{cement})=2.93

Specific gravity of fine aggregate(G_{fine})& coarse aggregate(G_{coarse})=2.65 & 2.82 respectively.

- Volume of Concrete = 1 m³
- Estimated air content = 2% volume of concrete

$$= 0.02 \text{ m}^3$$

- Volume of Cement = $\frac{M_{\text{cement}}}{G_{\text{cement}} \times \rho_{\text{water}}}$

$$= 0.161 \text{ m}^3$$

- Volume of Water = $\frac{M_{\text{water}}}{G_{\text{water}} \times \rho_{\text{water}}}$

$$= 0.158 \text{ m}^3$$

- Volume of Chemical Admixture = $\frac{M_{\text{ch.admixture}}}{G_{\text{ch.admixture}} \times \rho_{\text{water}}}$

- Mass of Chemical Admixture = 2% Mass of cement
= 9.438 kg

- Therefore, Volume of Chemical Admixture = 0.005 m³

- Volume of Total Aggregate = (1 - (0.02 + 0.161 + 0.158 + 0.005))
= 0.656 m³

- Mass of Coarse Aggregate = 1082.45 kg

- Mass of fine Aggregate = 721.60 kg

Table 4.1 show the quantity of each design mix materials in kg.

Total Volume = Volume of three cubes and volume of three molds

$$= 3 * (a^3 + \pi r^2 h)$$

$$= 3 * (0.15^3 + \pi * 0.05^2 * 0.2733)$$

$$= 0.01656 \text{ m}^3$$

$$\text{Take 75\% extra} = 1.75 * 0.01656$$

$$\text{Final volume required} = 0.028988 \text{ m}^3$$

All the contents of design mix was required to be obtained for a total volume of 0.28988 m³. 75 % extra volume was necessary to consider to balance out the wastage occur during the mix preparation.

Table 4.2 represents the design mix materials for 1 cum of concrete

Table 4.1 Calculated Design Mix for 1 cum of concrete

1	Cement Content	472 kg
2	Water	158 kg
3	Fine Aggregate	722 kg
4	Coarse Aggregate	1082 kg
	1) Coarse Aggregate(20mm)	649 kg
	2) Coarse Aggregate(10mm)	433 kg
5	Slump of Concrete	50 kg
6	Admixtures	9.44 kg

Table 4.2 Required Concrete contents for required volume

Cement	Water	Fine Aggregate	Coarse Aggregate 20	Coarse Aggregate 10	Admixture
14	5	21	19	13	0.16

4.4 Problems occur while casting the samples

Since the study aimed to develop a novel method for calculating the shear stress between the FRP-concrete interface, it was required to cutting the sample along a specified plane. Previous studies indicated that a plane inclined at 45° to the vertical face of the cylinder did not yield the necessary shear stress values. To obtain the maximum shear stress value, it was necessary to alter the angle of inclination. Consequently, for this study, an angle of 30° from the vertical face of the cylinder was selected as shown in Fig. 4.2. This adjustment was made to optimize the angle for better accuracy in measuring shear stress, ensuring that the study could precisely determine the shear stress values at the FRP-concrete interface. By choosing the 30° inclination, the study aimed to enhance the reliability of the measurements and provide more accurate data for evaluating the performance and interaction between FRP and concrete in reinforced structures.

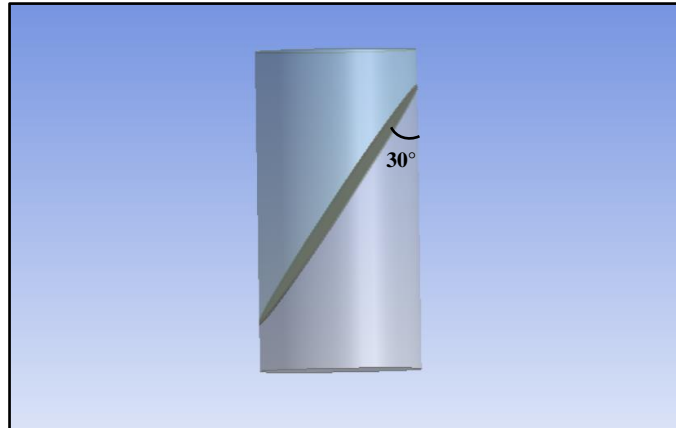


Fig. 4.2 Cylindrical Sample represent the required angle from vertical face of the cylinder

To cast the concrete sample in the required inclination angle, the base plate in core cutter machine should be inclined at 30° but the base plate is only come with preset angles of $0^\circ, 15^\circ, 30^\circ, 45^\circ$ from the base. The molds is required to be inclined at 30° from the vertical face, not from the base, so to avoid this problem, it has been decided to cut the PVC pipe in the required angle.

4.4.1 Preparation of Molds from PVC pipe

For the casting of cylindrical samples, a molds has to be prepared. PVC pipe of Internal diameter 100 mm has been taken for sample casting. The following steps are being followed for the preparation of molds

Step 1. First, the required marking had been done on the PVC pipe using a marker as shown in Fig. 4.3

Step 2. Secondly, For maintaining the stability, the PVC pipe is being held between two fix points. The marking of 30° is being done on the top surface of pipe with the help of protractor.

Step 3. Now, the hexa cutter, is being run in the marked direction, to obtained the required angle (Fig. 4.4) .precaution should be taken to maintain the stability of the PVC pipe while using the cutter.

Step 4. Repeat the same step (as above) in the bottom portion of the PVC pipe. The PVC pipes was cut in the required shape of molds as shown in Fig. 4.5

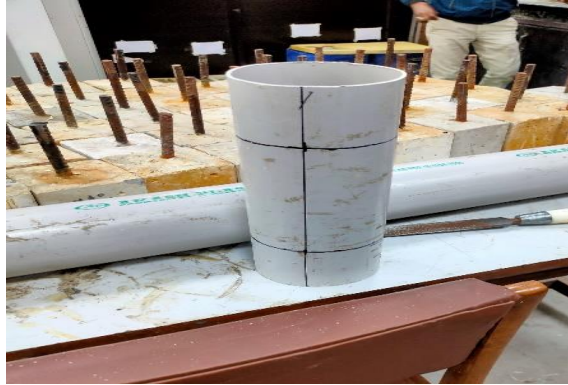


Fig. 4.3 Marking done on the PVC pipe



Fig. 4.4 Image showing the required plane of separation of molds after running the hexa blade

4.5 Learnings while casting the samples

To prepare the sample, the casting has to be done in a specific molds shape, whose one end has a horizontal surface and other end contain inclined surface as discussed earlier. The traditional casting process doesn't turn out to be required one. In the traditional process of casting, the prepared concrete mix is placed in the molds in three to four different layers, followed by tamping with a tamping rod. This process is followed till the molds is completely fill up by concrete mix.



Fig. 4.5 Image showing the different orientation of molds prepared from the PVC Pipe

After filling the concrete mix, it has been observed that the concrete started to flow from top surface after some time. This may occur due to several reasons like improper design mix, high temperature during casting, inadequate slump value (while calculating design mix), inclined surface of molds or insufficient compaction.

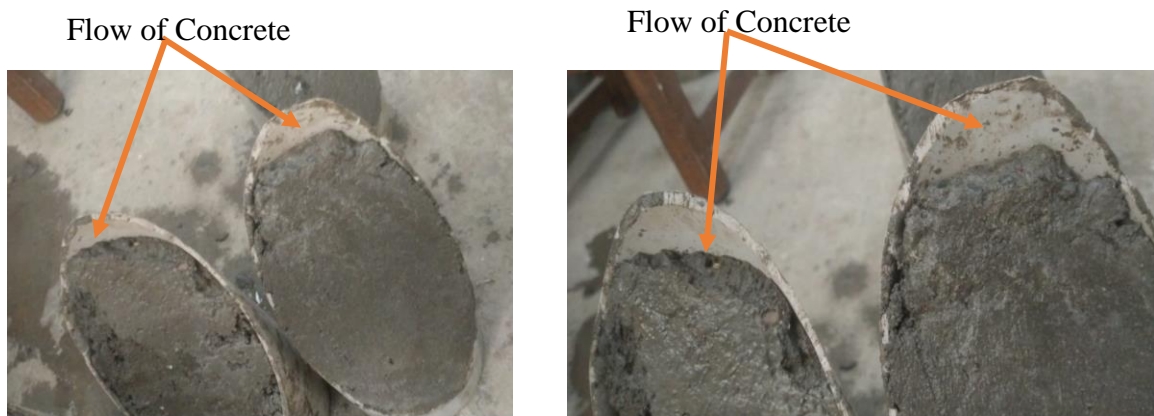


Fig. 4.6 Image represents the flow of concrete on the top surface of molds

To overcome this issue, a new design mix has been prepared for a slump value of 50 mm and the amount of admixture has been increased to 2% of mass of cement. For casting of sample, a pit has been dug out on the ground surface to avoid the concrete flow.



Fig. 4.7 Placing of molds in the pit with a flat plywood supported at the inclined surface

In the pit, the top(inclined) surface of the molds has been put towards the ground and horizontal surface of the molds is put towards the top, so that the the concrete flow towards the inclined surface effortlessly. The inclined surface has been cover with smooth plywood and joint between them has been cover with an adhesive like tape, so that concrete reside with in the molds. Proper tamping has been done in four different layers with the help of tamping rod.

After proper placing of the concrete in the molds, the sample has been taken out next day and the process of 28 days curing will start.

4.6 Lab Work for preparation of sample

4.6.1 Cylindrical Sample Preparation

4.6.1.1 Grinding of concrete surface

After the 28 days of curing, the sample is required to be ready for testing, for the proper joint of two concrete section, the grinding has to be done on the surface of concrete.



Fig. 4.8 Grinding machine used for leveling of surface



Fig. 4.9 Grinding operation done on the inclined concrete surface

After the grinding of inclined surface, the final surface looks like



Fig. 4.10 Surface obtained after grinding operation

4.6.1.2 Preparation of Epoxy mix

The epoxy type used is GOLDBOND® 1893-Saturant from *Krishna Conchem Products Pvt. Ltd.* Table 4.3 and Table 4.4 represents technical data sheet and mechanical properties of Epoxy respectively.

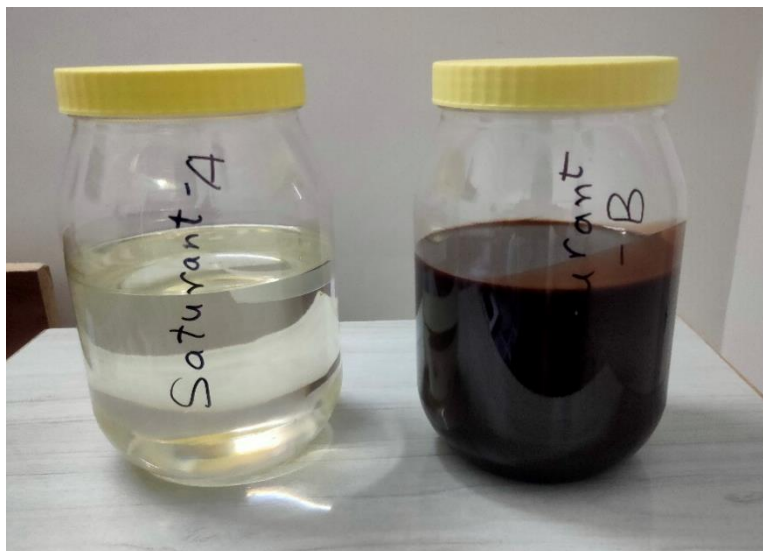


Fig. 4.11 Saturant-A(left one) and Saturant-B(Right one) of Epoxy

Table 4.3 Technical data sheet for Epoxy

Properties	Goldbond® 1893-Saturant
Base	Epoxide Resin
% Solids	100
Mix Proportion(By weight)	Part A(Base) Part B(Curing Agent) 1 1
Theoretical Coverage(on smooth concrete)for E-Glass Fiber	0.75-1.0 sq.mt/kg
Theoretical Coverage(on smooth concrete) for Carbon Fiber	1.5-2.0 sq. mt/kg
Pot Life	45 min at 30° C
Shelf Life	12 Months
Tack free Life	1-2 hours
Recommended no. of coats	2
Overcoat Time	30 min. to 3 hours between two coats of saturants
Packing	10 kg, 60 kg

Table 4.4 Different mechanical properties for Epoxy (Part A and Part B)

Cast Epoxy Material Properties		
Property	Method	Typical Test value
Compressive Strength	ASTM D-695	70 Mpa
Tensile Strength	ASTM D-638 Type-I	50 Mpa
Tensile Modulus	ASTM D-638 Type-I	3.2 Mpa
Elongation %	ASTM D-638 Type-1	5
Flexural Strength	ASTM D-790	>40 Mpa
Flexural Modulus	ASTM D-790	3.12 GPa

For the preparation of sample, the base and primer are required to be mix in proper ratio. According to Data Sheet, the required ratio is 1:1. Consider Fig. 4.12 for manual mixing of epoxy in the lab.

After weighing of Epoxy, proper mixing is required to de done. The mixing has to done for at least 10 minutes.

4.6.1.3 Fixation of Fiber Reinforced Polymer (FRP) Sheet

After the preparation of Epoxy mix, it has to be applied over the inclined concrete surface to fix the two FRP sheet of 5 cm wide as show in Fig. 4.13



Fig. 4.12 Manual mixing of two parts of Epoxy



Fig. 4.13 Application of Epoxy to the inclined surface of Concrete for fixation of FRP sheet

After applying the epoxy, the FRP sheet is meticulously positioned atop it to prevent the spread of epoxy glue. Following a 30-minute interval, a thin plastic sheet is placed over the FRP sheet, applying distributed load to ensure uniform bonding between the epoxy and the FRP sheet. Fig. 4.14 simply show the application of FRP on the epoxy wet layer.



Fig. 4.14 Image representing complete fixation of FRP sheet to concrete surface
 The material properties of FRP as shown in Table 4.5 is provided by the manufacturer is used in the numerical validation of data later.

Table 4.5 Material properties of FRP

Properties	CFRP laminates
Fiber Type	High Tensile Strength
Fiber weight(gm/m^2)	400
Density(gm/cm^3)	1.6
Design thickness(mm)	1.2
Ultimate strength(N/mm^2)	2900
Young Modulus strength(kN/mm^2)	165
Ultimate strain	17576
Poisson ratio	0.3
Bond stress between concrete and FRP(N/mm^2)	3.78

After the fixation process, the sample is left undisturbed for 24 hours to ensure the bond between the concrete surface and the FRP sheet is maintained as shown in Fig 4.15. Following this period, epoxy is applied atop the FRP sheet to facilitate the fixation of the another concrete component. After applying the epoxy,

the additional concrete component is carefully positioned atop it, and the entire assembly is left undisturbed for 24 to 48 hours.



Fig. 4.15 Complete assembly to provide lateral and longitudinal support to cylindrical specimen

4.6.2 Casting of Concrete Cube

Referring the design mix (Clause 4.3) , the three concrete cube samples are required to be cast.

4.6.2.1 Batching

Materials are batched using the *Equinox Electronic platform weighing scale*, followed by a manual dry mixing process.

4.6.2.2 Addition of water

The water and admixture, as calculated in the design mix, are added to the dry mix in three to five separate stages. The admixture needed to be thoroughly mixed with water before usage. Mixing is being done till the uniform consistency is being achieved.

4.6.2.3 Filling of concrete in molds

After properly mixing the concrete ingredients, it needs to be poured into molds. To begin this process, the molds are cleaned and oiled first. The mixture is then filled into the molds in three separate layers, with compaction performed for each layer. The top layer is slightly overfilled and smoothed with a trowel as shown in Fig. 4.16



Fig. 4.16 Concrete mix filled in cubical molds

After filling the molds, the samples are being allowed to set for at least 24 hours in the shade after then place the demolds cubes in a water bath at $27^{\circ}\text{C} \pm 2^{\circ}\text{C}$ for 28 days for the completion of the curing process.

4.7 Testing of samples

The process of testing concrete cubes and cylindrical samples is conducted using a compression testing machine. This essential procedure involves carefully placing the fully cured samples into the compression-testing apparatus. Once secured in place, a meticulously controlled and gradually increasing load is applied to the samples until they reach their breaking point. This systematic approach ensures a thorough evaluation of the compressive strength of the concrete specimens, providing crucial insights into their performance under stress and helping to inform engineering decisions with precision and reliability.

4.7.1 Testing of concrete cubes

Initially, the concrete samples are tested. The cured samples are taken out from the curing tank and left in an open environment for 1 hour before testing as shown in Fig. 4.17



Fig. 4.17 Concrete cubes taken out of curing tank for testing

Before testing the samples, the UTM is calibrated according to the manufacturer's instructions to maintain accuracy. The loading rate is set to 0.8 MPa/sec. After that, the concrete sample is placed inside the UTM as shown in Fig. 4.18 ,to facilitate the testing process.



Fig. 4.18 Placing of concrete cube sample in the UTM for testing

Next, the concrete samples are placed between the compression platens. The adjustable crosshead is positioned as required, and then the pressure valve is closed. The test is then started. When the sample is crushed(Fig. 4.19), the maximum peak load is recorded by the AIMIL UTM software.



Fig. 4.19 Crushed Concrete Sample

4.7.2 Testing of cylindrical specimens

The steps used for testing of concrete cubes and cylindrical samples are same (Fig. 4.29), only the difference is being the load rate is now reduced to 0.6 MPa/sec from 0.8 MPa/sec.



Fig. 4.20 Placing of cylindrical sample in the UTM for testing

After proper calibration of UTM Machine, the test was done. Fig 4.21 represents the sample condition ,when the peak was applied.



Fig. 4.21 Images show the slipping of two interfaces of cylindrical sample at peak level of load

4.8 Data Obtained from UTM

The result obtained are as follows

4.8.1

For Concrete Cubes

Table 4.6 Data obtained from UTM for cubical samples

Samples Parameters	Cubes		
	Peak Load,P(kN)	Area,A(mm ²)	Compressive strength(P/A) (N/mm ²)
1	785	22500	34.88
2	948	22500	42.13
3	939.09	22500	41.73
Average			39.58

4.8.2

For Cylindrical Samples

To analyze the data for cylindrical samples, the area of inclined surface (Fig. 4.22) and effective peak load (Fig. 4.23) has to be calculated, which is given below

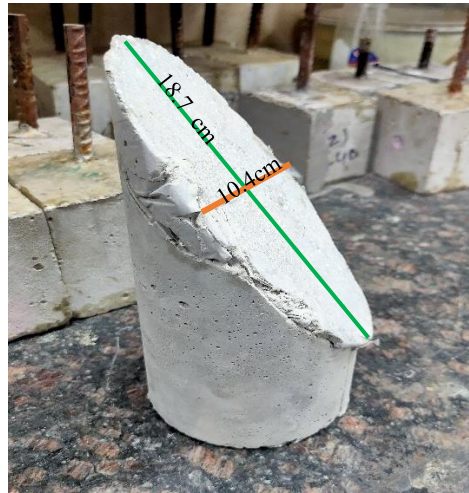


Fig. 4.22 Images shows dimension of major and minor axis of inclined surface

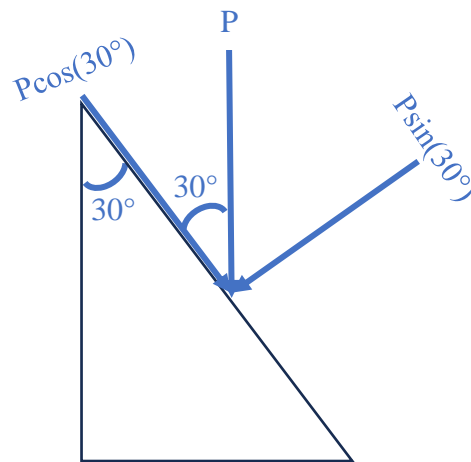


Fig. 4.23 Calculation of peak load

$$\begin{aligned}
 \text{Area of ellipse} &= \pi * a * b \\
 &= \pi * (18.7/2) * (10.4/2) \\
 &= 152.74 \text{ cm}^2 \\
 &= 15274 \text{ mm}^2
 \end{aligned}$$

Table 4.7 Data obtained from UTM for cylindrical samples

Samples		Cylinder		
Parameters	Peak Load,P(kN)	Area of Inclined Surface,A(mm ²)*	Effective load, P'(kN)	Stress=Effective Load/(2*Inclined area) (N/mm ²)
1	236	15274	204	7
2	142	15274	123	4
3	109	15274	94	3
Average				4.67

So, the obtained bond stress is 4.67 Mpa.

4.9 Validation of obtained experimental results with ANSYS software

Validation is essential in experimental research to confirm that the results are accurate, reliable, and reproducible under similar conditions. This section outlines the process of validating experimental results using ANSYS software, a robust tool for finite element analysis (FEA). This process entails comparing the experimental data with ANSYS simulation results to evaluate the accuracy and reliability of the findings.

4.9.1 Input data

Initially, the engineering data of materials need to be provided in the software. The compressive strength, Poisson's ratio, and Young's modulus of concrete are 39.6 MPa, 0.18, and 31,464 MPa, respectively. The data for epoxy and FRP are taken from Table (4.3,4.4) and 4.5 respectively.

4.9.2 Modelling

The modelling of the cylinder was carried out using the *Design Modeler* tab in ANSYS. The cylinder was specified to have a length of 273 mm and a diameter of 100 mm, as depicted in Figure 4.24. To facilitate the study, a plane inclined at 30° to the vertical face of the cylinder was modeled. An epoxy layer with a thickness of 0.5 mm was applied to this inclined plane. For the base of the model, the x-y plane was selected, with the z-axis serving as the altitude axis. When utilizing the slice command, the angle had to be chosen from the center of the cross-sectional area due to limitations within ANSYS software. This step ensured precise slicing along the desired plane of inclination. Once the modelling was complete, the obtained cylinder model was used

for further analysis. This included evaluating the shear stress distribution along the inclined plane and examining how the FRP and epoxy thickness influenced the interfacial shear stress between the FRP and concrete.

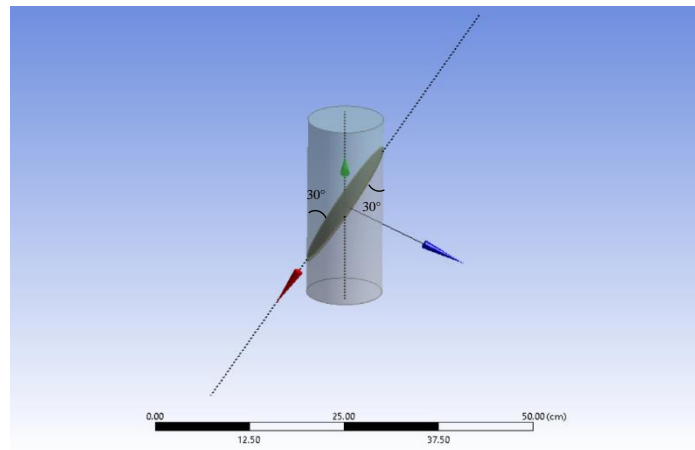


Fig. 4.24 Images represent cylindrical sample modelled in ANSYS

4.9.3 Analysis

The analysis part is done in the *Static Structural Mechanical* tab of the software. The mesh size selected is 6mm(Fig. 4.26). The top end of model is fixed and an uniform areal load of magnitude 20.68 MPa is applied from the bottom end(Fig. 4.25). The value 20.68 is calculated using the peak average load of 162 kN and bottom end area of cylinder as shown in Fig. 4.27

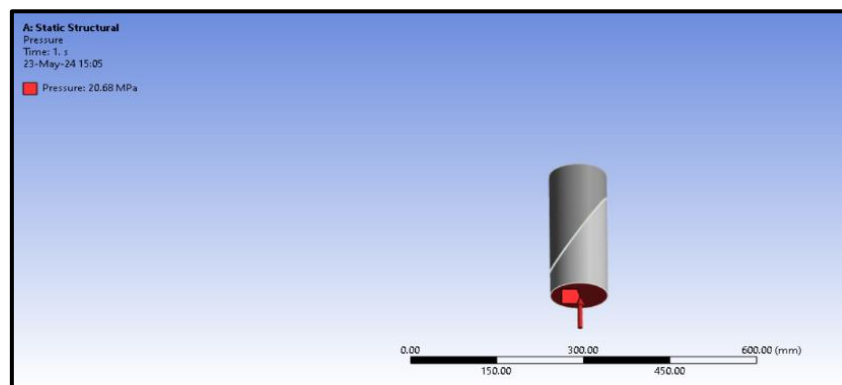


Fig. 4.25 Image represents uniform areal load (pressure) is applied at bottom end of the sample

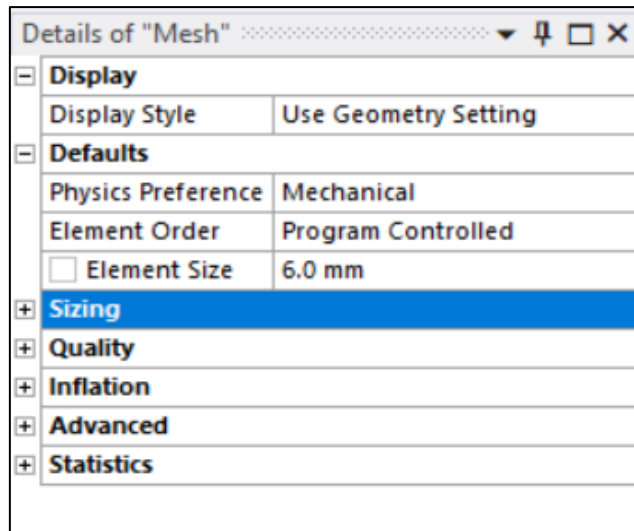


Fig. 4.26 Image represents Mesh properties

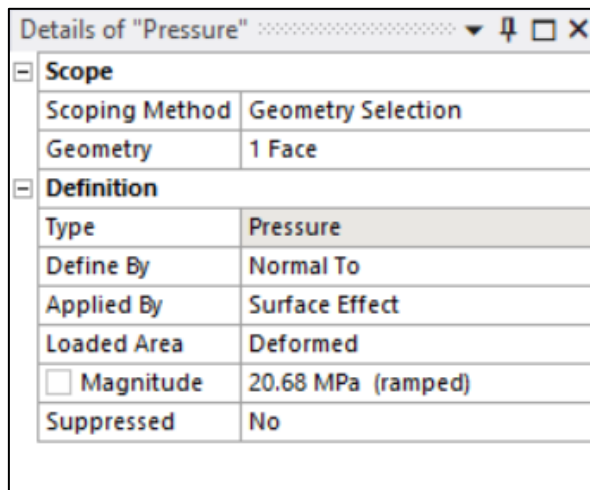


Fig. 4.27 Pressure application

4.9.4 Results obtained

The path line was defined along an inclined surface to facilitate detailed analysis. This path line served as a reference for measuring and evaluating the variation in shear stress along the inclined plane. Following the definition of the path line, the analysis was carried out using advanced computational techniques to assess the distribution of shear stress along this specified path.

The results of this analysis, including the various shear stress values and their corresponding distances along the inclined surface, are presented in Table 4.8.

This table provides a comprehensive set of data points that highlight how shear stress changes along the length of the inclined plane.

Additionally, a curve illustrating the relationship between shear stress and distance along the inclined surface from the right end is depicted in Figure 4.28. This graphical representation offers a visual interpretation of the data, showing the shear stress distribution in a clear and concise manner. The curve helps in understanding the trends and variations in shear stress, which are critical for evaluating the performance and structural integrity of the FRP-concrete interface

Table 4.8 Analysis data obtained from ANSYS Software

Serial No.	Distance [mm]	Value [MPa]
1	0	2.3394
2	4.1882	2.0922
3	8.3765	1.8375
4	12.565	1.6397
5	16.753	1.6157
6	20.941	1.6016
7	25.129	0.12237
8	29.318	0.1249
9	33.506	0.12477
10	37.694	0.12605
11	41.882	0.12706
12	46.071	0.1313
13	50.259	0.1318
14	54.447	0.13058
15	58.635	0.13319
16	62.824	0.13149
17	67.012	0.13674
18	71.2	0.14098
19	75.388	0.14134
20	79.577	0.13973
21	83.765	0.13914
22	87.953	0.13893
23	92.141	0.13762
24	96.33	0.13644

Serial no.	Distance [mm]	Value [MPa]
25	100.52	0.14002
26	104.71	0.14392
27	108.89	0.14878
28	113.08	0.14612
29	117.27	0.14559
30	121.46	0.14443
31	125.65	0.14686
32	129.84	0.15016
33	134.02	0.15907
34	138.21	0.1467
35	142.4	0.14111
36	146.59	0.14413
37	150.78	0.13903
38	154.97	0.13793
39	159.15	0.1355
40	163.34	0.13538
41	167.53	0.14156
42	171.72	0.13514
43	175.91	0.12925
44	180.09	0.12804
45	184.28	0.13386
46	188.47	5.594
47	192.66	5.4808
48	196.85	4.7674
49	201.04	2.4865

From the above table ,the maximum value of shear stress obtained is 5.594 Mpa.

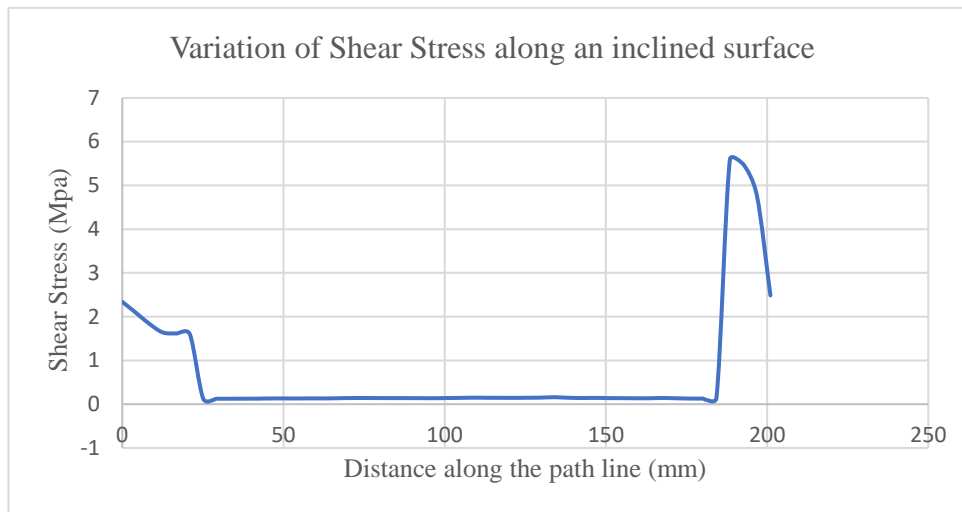


Fig. 4.28 Image represents the variation of shear stress along the inclined plane

4.9.5 Obtained Result Validation

The result obtained from the experimental study, which is **4.67 MPa**, closely matches the result from the numerical study, which is **5.594 MPa**. This demonstrates a strong correlation between the experimental and numerical findings. The slight difference between the two values occurs due to practical limitation in sample preparation, which indirectly indicating that the experimental results are reliable. Therefore, the experimental results are validated through this comparison with the numerical analysis.

4.10 Concluding remarks

1. The bond stress of 4.67 MPa indicates effective adhesion between the FRP and concrete, suggesting that the interface can withstand significant stress before failure.
2. The strength of the bond at 4.67 MPa contributes positively to the overall structural integrity of composite systems utilizing FRP and concrete, ensuring that the materials work together effectively under load.

3. For practical engineering applications, this bond stress value serves as a reference for designing FRP-reinforced concrete structures, ensuring safety and performance under expected load conditions

CHAPTER 5

NUMERICAL INVESTIGATION TO PERFORM PARAMETRIC STUDY FOR INTERFACIAL SHEAR STRESS BETWEEN FRP AND CONCRETE

5.1 General

The external bonding of fiber reinforced polymer (FRP) reinforcement to the surface of concrete members has become a widely adopted structural strengthening method due to the inherent advantages of FRP, such as its high tensile strength, low density, excellent corrosion resistance, high durability, and ease of installation (Chen et al. (2015)). Within the FRP strengthened reinforced concrete (RC) members, the interface between FRP and concrete often represents the weakest link, thereby playing a critical role in ensuring the efficacy of this strengthening technique (Aprile et al. (2001); Chen and Teng (2001)). The ultimate stage of FRP-strengthened members is frequently determined by various types of debonding failures. The behaviour of the interfacial bond between FRP and concrete significantly influences the performance of FRP-strengthened RC structures. Numerous research studies have been conducted and several interfacial bond-slip models have been proposed for FRP-to-concrete joints. Current investigations into bond-slip modelling can be broadly categorized into three groups (Zhou et al. (2010)) (a).Direct experimental methods, which involve directly measuring a bond-slip curve from test results (Carrara et al. (2011); Ferracuti et al. (2007); Ko and Sato (2007)).(b) Indirect experimental methods, which derive bond properties from test results using analytical solutions (Dai et al. (2005);Liu and Wu (2012)).(c).Finite-element (FE) analysis (Kamel, A.M.S.,(2003);Lu et al. (2005);Lu et al. (2006)).

The finite element method (FEM) emerges as a valuable tool for investigating FRP debonding failures. While laboratory experiments using strain gauges struggle to accurately predict interfacial stress distributions in FRP-strengthened beams due to the compacted variation of stress, particularly post-concrete cracking where crack locations are typically unknown beforehand, FEM offers a more

reliable alternative. Consequently, several research groups have turned to FEM to analyse debonding failures in FRP-strengthened RC beams (Chen et al. (2012); Chen et al. (2011); Yang et al. (2003); Niu and Wu (2005); Niu et al. (2006); Niu and Karbhari (2008)).

5.2 Problems

In finite element (FE) modelling studies focusing on debonding failures (Chen et al. (2012); Chen et al. (2011)) it was recognized that two elements are crucial for accurately simulating debonding failure and the complete debonding process precise modelling of localized concrete cracking behaviour and accurate representation of the interfacial bond-slip behaviour between concrete and both internal steel and external FRP reinforcements. However, incorporating these elements into the FE approach was found to result in significant convergence challenges in during the later loading stages when conventional solution techniques, such as the load or displacement control Newton–Raphson method and the arc-length method, were employed to solve the nonlinear static problem. These difficulties primarily arise from severe nonlinearities induced by strain softening phenomena like concrete cracking and interfacial debonding between concrete and FRP/steel reinforcement. To address these challenges, empirical solution techniques like line searches may be utilized (Niu and Karbhari (2008)), although the effectiveness of such approaches typically varies depending on the specific problem due to their empirical nature.

5.3 Finite-Element Analysis and Implementation

For the study, a concrete cylinder of height 195 mm and diameter 100 mm are modelled in the ANSYS as shown in Fig 5.1. The entire geometry is assumed to be linear elastic during the loading process. Different thicknesses of epoxy are being applied in the model corresponding to a particular layer of FRP. Mechanical properties of Concrete, Epoxy and FRP are given in Table 5.1

For the analysis, a plane at a height of 10 cm from the base of cylinder is being selected for the application of FRP and Adhesive. Plane is making an angle of 35° from the vertical face of cylinder (as shown in Fig. 5.1).

Table 5.1 Materials properties

Materials/Properties	Density(kg/m ³)	Young Modulus (GPa)	Poisson's Ratio	Ultimate Tensile Strength (MPa)
Concrete	24	30	0.18	NA
FRP	1600	165	0.30	2900
Epoxy	1250	3.227	0.37	30.70

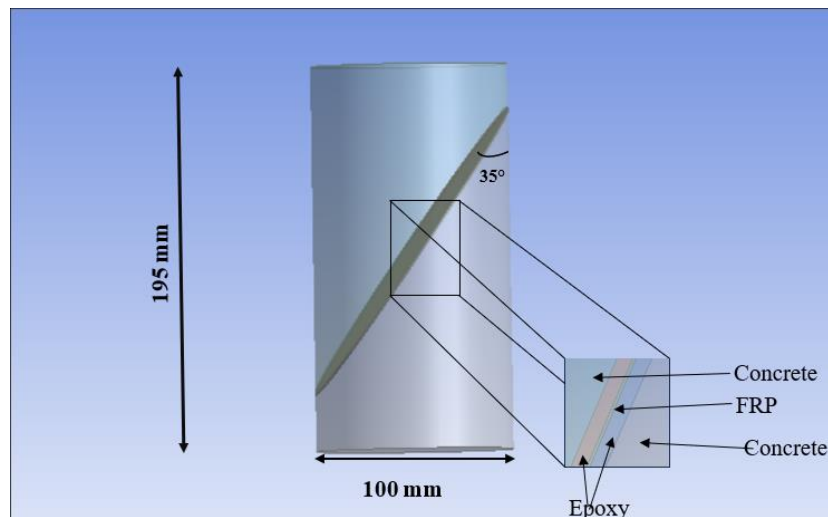


Fig. 5.1 Cylindrical Model with FRP at inclined surface

Different thicknesses of FRP (T_f) and Epoxy (T_e) were used for the parametric study, as shown in the Table 5.2. This study aimed to understand how varying the thicknesses of these materials affects the bond stress and overall performance of the FRP-concrete interface.

5.3.1 Numerical Modelling

The numerical modelling is done in the ANSYS software. The finite element model of the cylinder consists of a uniform mesh size. The element size being taken is 2.0 mm having 82174 nodes & 17562 elements. The physics preference used in the meshing is mechanical and element order is program controlled, refer Fig. 5.2(a)

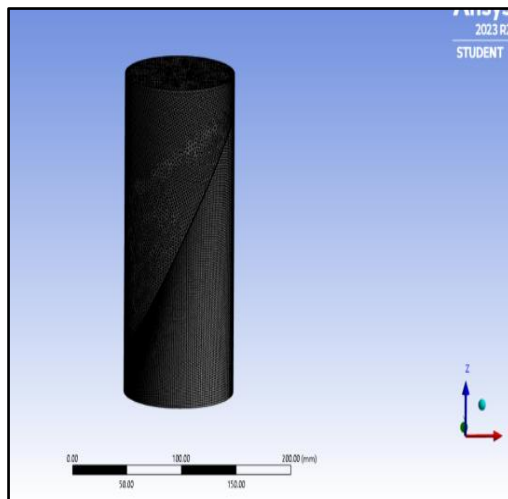
and Fig. 5.2(b) For the analysis, the bottom face of the cylinder is fixed and a point load of 20N is applied in the top face, in the (-z) direction as shown in Fig. 5.3

Table 5.2 Different combination of FRP and Epoxy Thickness

$T_f(\text{mm})$	$T_e(\text{mm})$	$T_e(\text{mm})$	$T_e(\text{mm})$	$T_e(\text{mm})$
0.10	0.5	1.0	1.5	2.0
0.15	0.5	1.0	1.5	2.0
0.20	0.5	1.0	1.5	2.0

In the Finite Element modelling, there are four interfaces namely (a). Between top concrete & top epoxy i.e. plane 1 (b). Between top epoxy and FRP i.e. plane 2 (c.) Between FRP and bottom epoxy i.e plane 3 (d.) Between bottom epoxy and bottom concrete i.e. plane 4. Refer Fig. 5.4 for understanding of different interfaces.

To find the interface which gives maximum shear stress, an analysis is being carried out on a typical interface having a $T_f=0.10$ mm and $T_e=0.5$ mm.



(a)

Display	
Display Style	Use Geometry Setting
Defaults	
Physics Preference	Mechanical
Element Order	Program Controlled
<input type="checkbox"/> Element Size	2.0 mm
Sizing	
Use Adaptive Sizing	Yes
Resolution	Default (2)
Mesh Defeaturing	Yes
<input type="checkbox"/> Defeature Size	Default
Transition	Fast
Span Angle Center	Medium
Initial Size Seed	Assembly
Bounding Box Diagonal	240.88 mm
Average Surface Area	12400 mm ²
Minimum Edge Length	314.16 mm
Quality	
Check Mesh Quality	Mesh Quality Worksheet
Error Limits	Aggressive Mechanical
<input type="checkbox"/> Target Element Quality	Default (5.e-002)
Smoothing	High
Mesh Metric	None

(b)

Fig. 5.2 (a) FE Model represent mesh size (b) Mesh properties

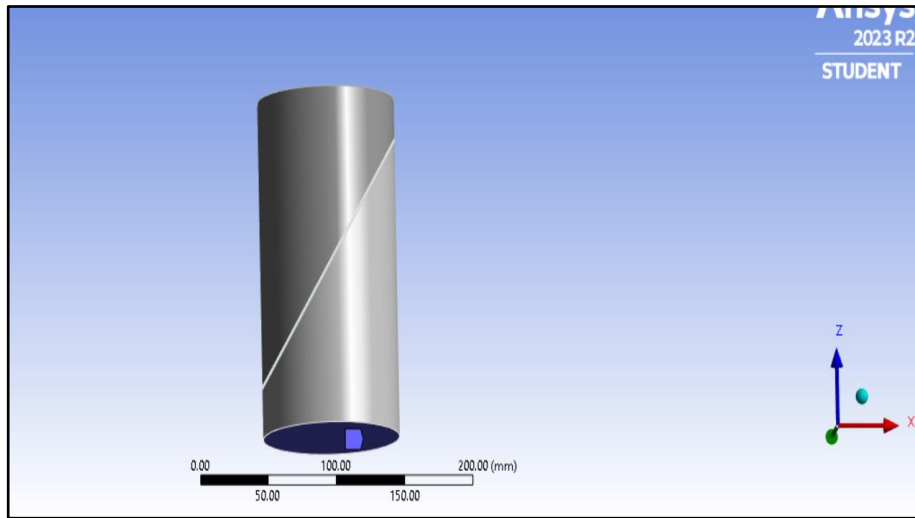


Fig. 5.3 Finite Element Model represents boundary conditions

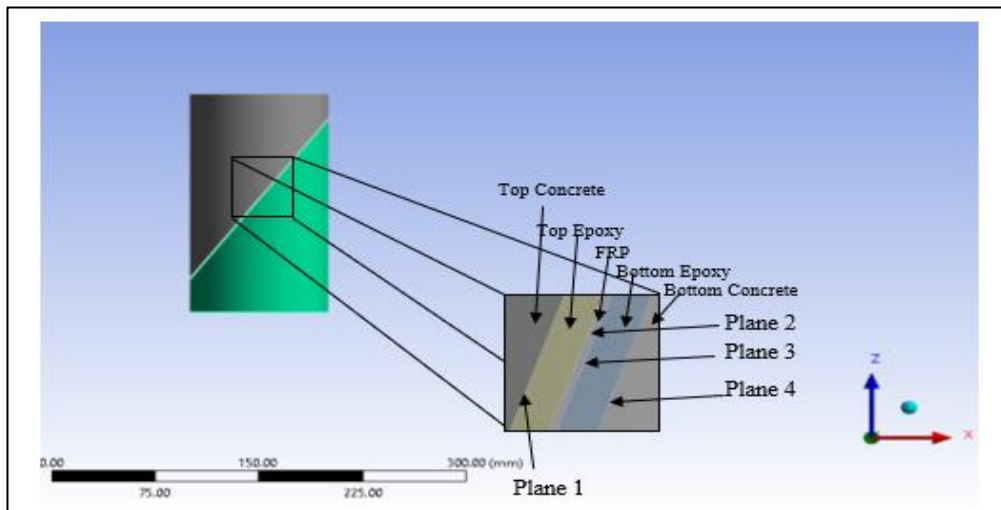


Fig. 5.4 Geometry for obtaining plane of maximum shear stress

5.4 Results from Analysis

After carrying out the analysis in the typical plane, the shear stress corresponding to different planes are shown in Table 5.3 and Fig. 5.5

Table 5.3 Stresses in different planes

Planes	Shear Stress(N/m ²)
1	1277
2	4395.7
3	1448.1
4	1440.5

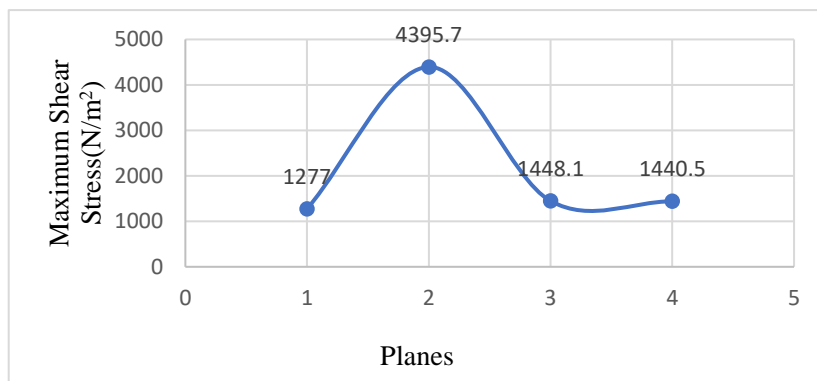


Fig. 5.5 Graph represents shear stress variation in different planes

From the above curve, it becomes clear that the maximum shear stress is obtained in plane 2. Therefore, plane 2 is used as a reference for further analysis. As per detailed in Table 5.2, a study is conducted to determine the maximum shear stress with various combinations of FRP and epoxy thicknesses. The results of this analysis are presented in Table 5.4.

Different combinations of FRP and epoxy thicknesses are selected based on practical considerations commonly employed in the retrofitting of structures. By systematically varying the thicknesses, the study aims to identify the optimal configurations that maximize shear stress resistance and enhance the performance of the FRP-concrete interface. This approach ensures that the findings are applicable to real-world scenarios, providing valuable insights for engineers involved in the design and retrofitting of FRP-reinforced structures

Table 5.4 Maximum shear stress with respect to different thickness of Epoxy and FRP

Epoxy Thickness, T_e (mm)	Maximum Shear Stress (Mpa)		
	For $T_f=0.10$ (mm)	For $T_f=0.15$ (mm)	For $T_f=0.20$ (mm)
0.5	4.40E-03	4.92E-03	4.86E-03
1.0	5.17E-03	5.46E-03	4.61E-03
1.5	5.84E-03	5.85E-03	4.98E-03
2.0	6.61E-03	6.31E-03	5.63E-03

5.4.1 Contours obtained for different thickness of FRP

The variation of shear stress along a plane is shown in the contour (refer Fig. 5.6,5.7,5.8) below. The variation is consider for maximum thickness of epoxy which is 2.0 mm. The red and blue color in contour represents the maximum and minimum value of stresses along the plane.

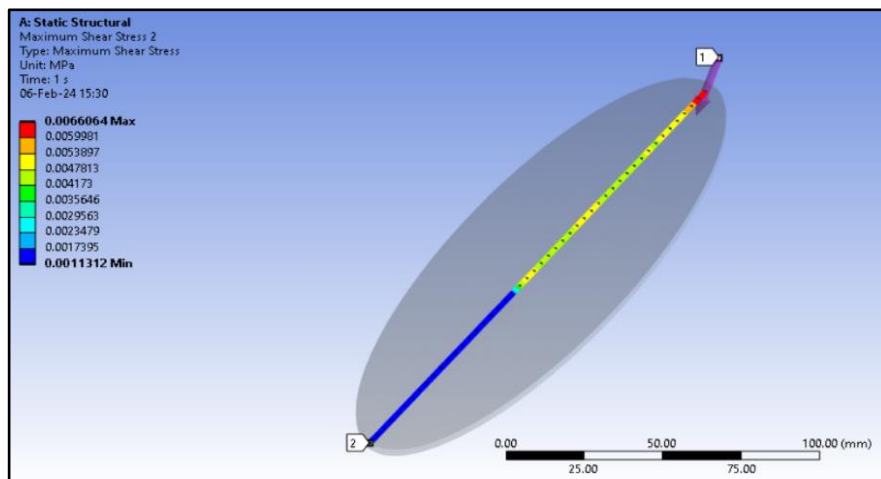


Fig. 5.6 Contour showing the shear stress variation in plane 2, when $T_f=0.10$ mm and $T_e=2.0$ mm

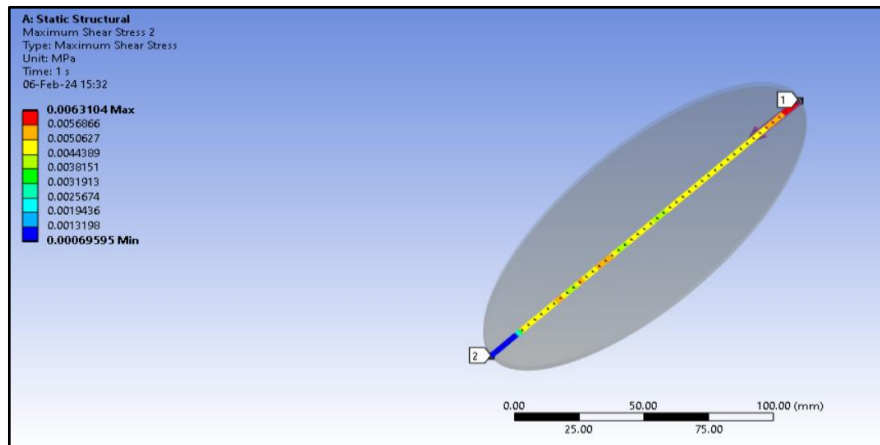


Fig. 5.7 Contour showing the shear stress variation in plane 2, when $T_f=0.15$ mm and $T_e=2.0$ mm

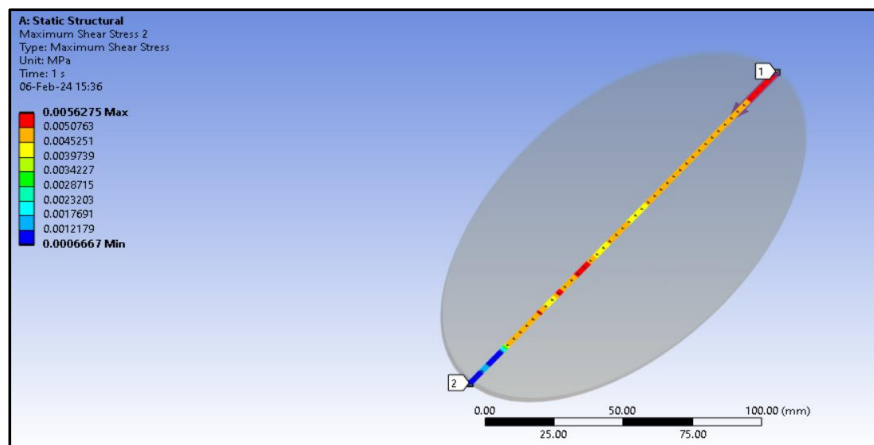


Fig. 5.8 Contour showing the shear stress variation in plane 2, when $T_f=0.20$ mm and $T_e=2.0$ mm

5.4.2 Curves obtained for different thickness of FRP and Epoxy

The curves obtained for different thicknesses of FRP and epoxy, as shown in Fig. 5.9, 5.10, and 5.11, illustrate the variation of shear stress along a specific plane, referred to as plane 2 (the plane between the top epoxy layer and the FRP). These figures depict how the shear stress distribution changes with different material thicknesses, providing valuable insights into the mechanical behaviour at the interface.

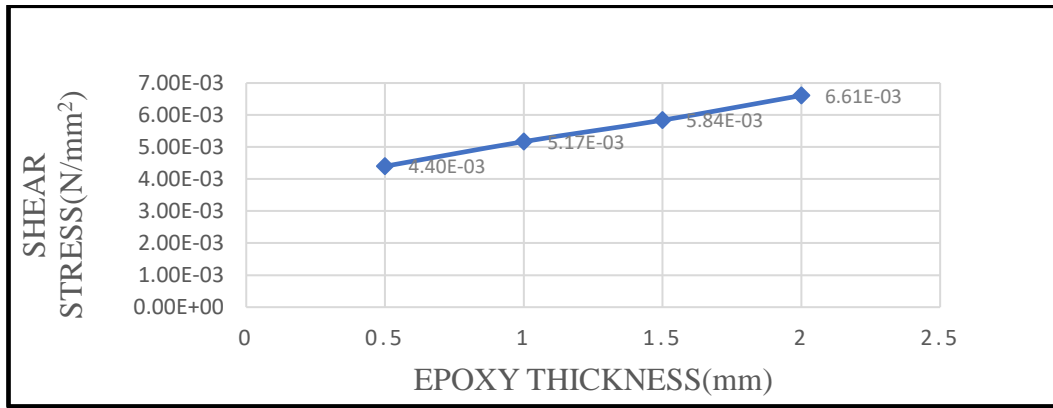


Fig. 5.9 Curve between Shear Stress and Epoxy Thickness, for $T_f=0.10$ mm

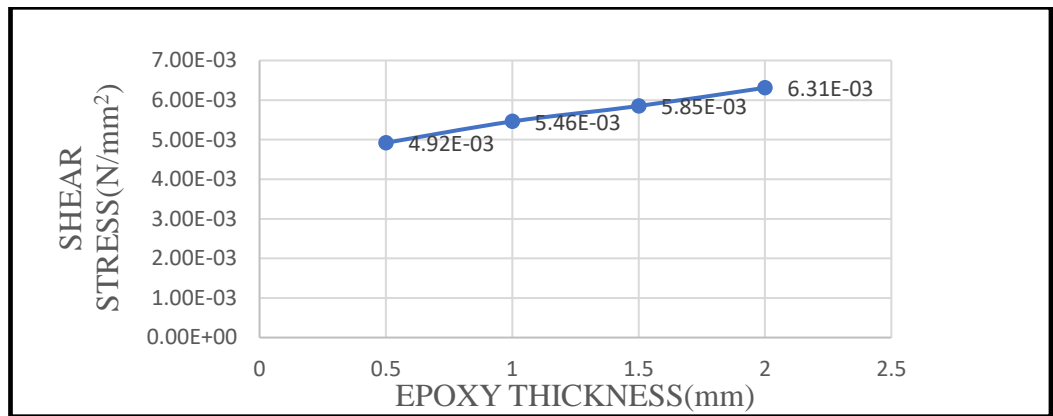


Fig. 5.10 Curve between Shear Stress and Epoxy Thickness, for $T_f=0.15$ mm

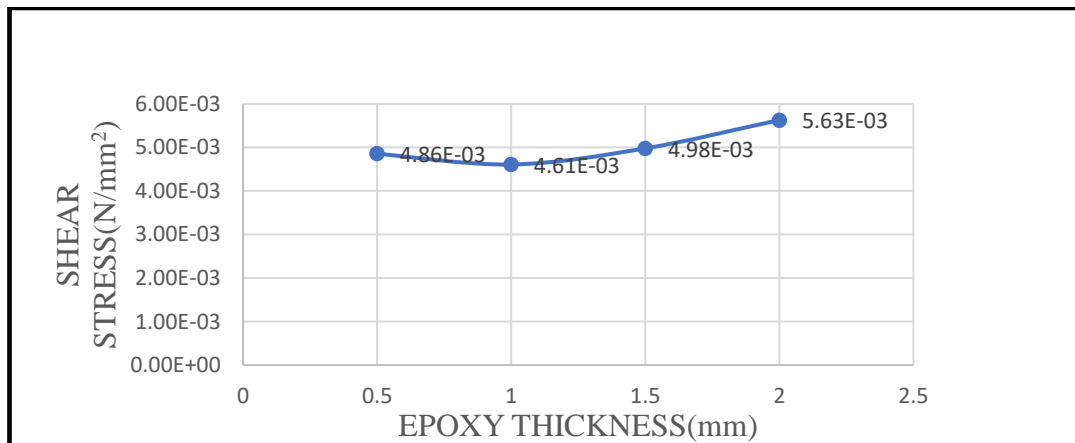


Fig. 5.11 Curve between Shear Stress and Epoxy Thickness, for $T_f=0.20$ mm

5.5 Concluding remarks

In this chapter, a numerical parametric study was conducted to investigate the variation of shear stress along the inclined plane of a cylinder. The geometry was modelled using ANSYS software, a powerful tool for finite element analysis. This study aimed to understand how different parameters influence the shear stress distribution on the inclined plane, which is an important aspect in retrofitting of structures subjected to complex loading conditions. Based on the findings of this study, the following conclusions were drawn

1. The value of maximum shear stress is obtained in plane 2, i.e., the interface between the top epoxy and FRP.
2. The value of maximum shear stress increases with the thickness of the epoxy layer.
3. The maximum shear stress is $6.61\text{E-}03$ MPa for $T_f = 0.10$ mm with $T_e = 2.0$ mm.
4. Along the plane, maximum shear stress is localized at the extreme right end of the plane.

CHAPTER 6

CONCLUSIONS AND FUTURE WORK

6.1 Summary

The objectives were established following an extensive review of the available literature on various experimental methods for calculating the bond stress between FRP and concrete. This comprehensive literature review formed the basis for identifying gaps and limitations in previous studies for the calculation of bond stress.

Chapter 2 of this thesis presents a detailed explanation of the relevant literature, organized into various sections. Including these sources contributes to the overall knowledge base and theoretical framework supporting this research.

In Chapter 3, the capacity of the beam in flexure is calculated using the analytical method provided by ACI 440.2R-2017. The behaviour of the beam in flexure also helps to establish its relationship with the bond stress.

Chapter 4 primarily deals with the experimental work. Since traditional methods for calculating bond stress are complex and time-consuming, research is being conducted to develop a novel and simple method that can be easily performed using a Universal Testing Machine (UTM). The test specimens were cast using PVC pipe molds and were prepared using cement, aggregate (both fine and coarse), FRP, and epoxy. The experimental design includes information about the raw materials used, the preparation of test specimens, the equipment employed, and the techniques performed during the experiment. These experimental details lay the groundwork for further analysis and interpretation of the data.

In practical scenarios where retrofitting is done on any part of a building, the thickness of epoxy and FRP is not fixed, as there is no standard code governing the thickness of these two materials. Therefore, it becomes necessary to study the variation in bond stress when the thickness of epoxy and FRP is changed accordingly. Chapter 5 of this work considers such parameters for study the bond stress.

6.2 Conclusions

The various conclusion drawn from the above studies are

- It has been observed from the study that by applying an FRP (Fiber Reinforced Polymer) sheet with a thickness of 4.04 mm to the soffit (the underside) of the beam, the flexural capacity of the beam can be improved by 8.60%. This enhancement in flexural capacity indicates a significant improvement in the beam's ability to resist bending and deformation under load. The FRP sheet effectively increases the tensile strength of the beam, providing additional reinforcement where it is most needed.
- The study has revealed that the thickness of the FRP (Fiber Reinforced Polymer) sheet plays a crucial role in enhancing the flexural capacity of beams. However, this enhancement is not linear, meaning that the relationship between the FRP thickness and the flexural capacity does not increase in a straightforward, proportional manner.
- From the study, it has been found out that beam flexural capacity is directly depend upon it's section modulus. When an FRP sheet is applied to the beam, particularly on the tension side (such as the soffit), it effectively increases the distance between the outermost fibers in the cross-section and the neutral axis. This increased distance enhances the section modulus, which indirectly results in increase in flexural capacity.
- From the study, it has been found that in a cylindrical specimen, the maximum shear stress occurs on the plane lying between the top epoxy and the FRP (Fiber Reinforced Polymer) sheet. This finding helps to figure out the critical plane of failure. The maximum shear stress is concentrated in this interface due to many factors which include material property differences, load transfer mechanism and bonding quality.
- The bond stress of 4.67 MPa as obtained from the experimental study indicates effective adhesion between the FRP and concrete, suggesting that the interface can withstand significant stress without failure. This value of bond stress

demonstrates that the FRP (Fiber Reinforced Polymer) and concrete are securely bonded, capable of transferring loads efficiently between the two materials. The ability to resist a bond stress of 4.67 MPa without debonding or failure implies that the interface has a high level of mechanical integrity, essential for the composite system's structural performance.

- The study has found that the value of maximum shear stress increases with the thickness of the epoxy layer. This observation is crucial for understanding the behaviour of composite beams reinforced with Fiber Reinforced Polymer (FRP) and the role of the epoxy layer in stress distribution and structural performance. The value of bond stress for epoxy thickness of 0.5 mm is 4.40E-03, which further increases to 6.61E-03 for an epoxy thickness of 2.0 mm.
- In a cylindrical specimen, the numerical study implies that the shear stress increases towards the right side of the inclined plane. This observation is significant because it helps researchers to identify the critical position where shear failure is most likely to occur.

6.3 Future Scope

The future scope of research in bond stress calculation offers exciting opportunities for advancements and knowledge expansion. This section highlights potential areas for exploration to address current limitations and contribute to the development of innovative solutions.

- One avenue for exploration involves the development of novel experimental techniques (other than this study) for directly measuring interfacial shear stress with higher resolution and sensitivity. This may include advancements in microscopy techniques, such as atomic force microscopy or scanning electron microscopy, as well as the integration of advanced imaging technologies with mechanical testing apparatus.
- Additionally, there is also a potential scope for the refinement and validation of computational models and simulations to predict interfacial shear stress accurately across different length scales and material systems. This could

involve the utilization of multi-scale modeling approaches that incorporate molecular-level interactions, microstructural features, and macroscopic behavior to capture the complex interfacial phenomena influencing shear stress.

- Furthermore, this study can be expanded to include various exposure conditions, environmental factors, and humidity levels. By investigating bond stress under different scenarios, such as varying temperatures, moisture levels, and atmospheric conditions, researchers can gain a more comprehensive understanding of how these factors influence the performance and durability of materials. This broader scope will help develop more robust and versatile applications for bond stress calculations, ensuring reliability and effectiveness across diverse real-world conditions.
- Lastly, there is increasing interest in applying machine learning and artificial intelligence techniques to analyse experimental data, identify patterns, and optimize experimental parameters for more efficient and accurate determination of interfacial shear stress. By leveraging interdisciplinary approaches and fostering collaboration across various scientific disciplines, researchers can enhance the understanding of interfacial shear stress and its implications for material performance, structural integrity, and engineering design.

REFERENCES

1. ACI (440.2R) 2017 “Guide for the Design and Construction of Externally Bonded FRP Systems for Strengthening Concrete Structures”, American Concrete Institute, Farmington Hills, Washington
2. Aidoo, J., Harries, K.A. and Petrou, M.F., 2006. Full-scale experimental investigation of repair of reinforced concrete interstate bridge using CFRP materials. *Journal of Bridge Engineering*, 11(3), pp.350-358.
3. Aprile, A., Spacone, E. and Limkatanyu, S., 2001. Role of bond in RC beams strengthened with steel and FRP plates. *Journal of structural Engineering*, 127(12), pp.1445-1452.
4. Arruda, M.R., Firmo, J.P., Correia, J.R. and Tiago, C., 2016. Numerical modelling of the bond between concrete and CFRP laminates at elevated temperatures. *Engineering Structures*, 110, pp.233-243.
5. Barnes, R. A., Baglin, P. S., Mays, G. C., and Subedi, N. K. (2001). “External steel plate systems for the shear strengthening of reinforced concrete beams.” *Engineering Structures*, Elsevier, 23(9), 1162–1176.
6. Bilotta, A., DI Ludovico, M. and, and Nigro, E. (2009). “Influence of effective bond length on FRP-concrete debonding under monotonic and cyclic actions.” *9th International Symposium on Fiber Reinforced Polymer Reinforcement for Concrete Structures (FRPRCS-9)*, Australia.
7. Bizindavyi, L., and Neale, K. W. (1999). “Transfer lengths and bond strengths for composites bonded to concrete.” *Journal of Composites for Construction*, ASCE, 3(4), 153–160.
8. Blanksvärd, T., Täljsten, B., and Carolin, A. (2009). “Shear Strengthening of Concrete Structures with the Use of Mineral-Based Composites.” *Journal of Composites for Construction*, 13(1), 25–34.
9. Bonacci, J.F. and Maalej, M., 2000. Externally bonded FRP for service-life extension of RC infrastructure. *Journal of Infrastructure systems*, 6(1), pp.41-51.
10. Camli, U. S., and Binici, B. (2007). “Strength of carbon fiber reinforced polymers bonded to concrete and masonry.” *Construction and Building Materials*, 21(7), 1431–1446.
11. Carrara, P., Ferretti, D., Freddi, F. and Rosati, G., 2011. Shear tests of carbon fiber plates bonded to concrete with control of snap-back. *Engineering Fracture Mechanics*, 78(15), pp.2663-2678.
12. Ceroni, F., 2017. Bond tests to evaluate the effectiveness of anchoring devices for CFRP sheets epoxy bonded over masonry elements. *Composites Part B: Engineering*, 113, pp.317-330.
13. Ceroni, F., Ianniciello, M. and Pecce, M., 2016. Bond behavior of FRP carbon plates externally bonded over steel and concrete elements: Experimental outcomes and numerical investigations. *Composites Part B: Engineering*, 92, pp.434-446.
14. Chajes, M.J., Finch, W.W. and Thomson, T.A., 1996. Bond and force transfer of composite-material plates bonded to concrete. *Structural Journal*, 93(2), pp.209-217.
15. Chen, C., Wang, X., Sui, L., Xing, F., Chen, X. and Zhou, Y., 2019. Influence of FRP thickness and confining effect on flexural performance of HB-strengthened RC beams. *Composites Part B: Engineering*, 161, pp.55-67.

16. Chen, G.M., Chen, J.F. and Teng, J.G., 2012. On the finite element modelling of RC beams shear-strengthened with FRP. *Construction and Building Materials*, 32, pp.13-26.
17. Chen, G.M., Teng, J.G. and Chen, J.F., 2011. Finite-element modeling of intermediate crack debonding in FRP-plated RC beams. *Journal of composites for construction*, 15(3), pp.339-353.
18. Chen, G.M., Teng, J.G., Chen, J.F. and Xiao, Q.G., 2015. Finite element modeling of debonding failures in FRP-strengthened RC beams A dynamic approach. *Computers & Structures*, 158, pp.167-183.
19. Chen, J.F. and Teng, J.G., 2001. Anchorage strength models for FRP and steel plates bonded to concrete. *Journal of structural engineering*, 127(7), pp.784-791.
20. Dai, J., Ueda, T. and Sato, Y., 2005. Development of the nonlinear bond stress–slip model of fiber reinforced plastics sheet–concrete interfaces with a simple method. *Journal of composites for construction*, 9(1), pp.52-62.
21. Dai, J.G. and Ueda, T., 2003. Local bond stress slip relations for FRP sheets-concrete interfaces. In *Fiber-Reinforced Polymer Reinforcement for Concrete Structures (In 2 Volumes)* (pp. 143-152).
22. Ferracuti, B., Savoia, M.A.Z.Z.O.T.T.I. and Mazzotti, C., 2007. Interface law for FRP–concrete delamination. *Composite structures*, 80(4), pp.523-531.
23. Guo, Z.G., Cao, S.Y., Sun, W.M. and Lin, X.Y., 2005, December. Experimental study on bond stress-slip behaviour between FRP sheets and concrete. In *FRP in construction, proceedings of the international symposium on bond behaviour of FRP in structures* (pp. 77-84).
24. Heiza, K., Nabil, A., Meleka, N., and Tayel M. (2014). “State-of-the Art Review Strengthening of Reinforced Concrete Structures - Different Strengthening Techniques.” *Sixth International Conference on NANO-TECHNOLOGY IN CONSTRUCTION (NTC 2014)*, Volume 6.
25. Hemaanitha, R., and Kothandaraman, S. (2014). “Materials and methods for retrofitting of RC beams-A Review.” *International Journal of Civil Engineering and Technology (IJCIET)*, 5(3), 1–14.
26. Hussain, M., Sharif, A., Baluch, I. A., H., B. M., and AL-Sulaimani, G. J. (1995). “Flexural Behavior of Precracked Reinforced Concrete Beams Strengthened Externally by Steel Plates.” *ACI Structural Journal*, 92(1), 14–23.
27. Jumaat, M. Z., and Alam, M. A. (2009). “Strengthening of R.C. Beams Using Externally Bonded Plates and Anchorages.” *Australian Journal of Basic and Applied Sciences*, 3(3), 2207–2211.
28. Kamel, A.M.S., 2003. Experimental and numerical analysis of FRP sheets bonded to concrete.
29. Kanakubo, T., Tomoki Furuta, K. T., and Takeshi Nemoto. (2005). “Sprayed Fiber-Reinforced Polymers for Strengthening of Concrete Structures.” *Proceedings of the International Symposium on Earthquake Engineering Commemorating Tenth Anniversary of the 1995 Kobe Earthquake*, Volume 2 C-299-307, Volume 2, 299–307.
30. Keller, T., 2002. Overview of fiber-reinforced polymers in bridge construction. *Structural engineering international*, 12(2), pp.66-70.
31. Ko, H. and Sato, Y., 2007. Bond stress–slip relationship between FRP sheet and concrete under cyclic load. *Journal of Composites for Construction*, 11(4), pp.419-426.
32. Kumar,P.,(2021). “Study on reinforced concrete(RC) beams flexurally strengthened with carbon and aramid fiber reinforced polymer(FRP) strand sheets”(Doctoral dissertation, IIT Delhi)

33. Larralde, J., Elpert, M.S. and Weckermann, D., 2001. A simplified shear test for the adhesion of FRP composites to concrete. *Cement, Concrete, and Aggregates*, 23(1), pp.66-70.
34. Liu, K. and Wu, Y.F., 2012. Analytical identification of bond–slip relationship of EB-FRP joints. *Composites Part B Engineering*, 43(4), pp.1955-1963.
35. López-González, J.C., Fernández-Gómez, J. and González-Valle, E., 2012. Effect of adhesive thickness and concrete strength on FRP-concrete bonds. *Journal of Composites for Construction*, 16(6), pp.705-711.
36. Lu, X.Z., Jiang, J.J., Teng, J.G. and Ye, L.P., 2006. Finite element simulation of debonding in FRP-to-concrete bonded joints. *Construction and building materials*, 20(6), pp.412-424.
37. Lu, X.Z., Teng, J.G., Ye, L.P. and Jiang, J.J., 2005. Bond–slip models for FRP sheets/plates bonded to concrete. *Engineering structures*, 27(6), pp.920-937.
38. Lu, X.Z., Ye, L.P., Teng, J.G. and Jiang, J.J., 2005. Meso-scale finite element model for FRP sheets/plates bonded to concrete. *Engineering structures*, 27(4), pp.564-575.
39. Malek, A.M., Saadatmanesh, H. and Ehsani, M.R., 1998. Prediction of failure load of R/C beams strengthened with FRP plate due to stress concentration at the plate end. *Structural Journal*, 95(2), pp.142-152.
40. Nakaba, K., Kanakubo, T., Furuta, T., and Yoshizawa, H. (2001). “Bond behavior between fiber-reinforced polymer laminates and concrete.” *ACI Structural Journal*, 98(3), 359–367.
41. Neale, K.W., 2000. FRPs for structural rehabilitation a survey of recent progress. *Progress in structural engineering and materials*, 2(2), pp.133-138.
42. Niu, H. and Karbhari, V.M., 2008. FE investigation of material and preload parameters on FRP strengthening performance of RC beams, I model development. *Journal of Reinforced Plastics and Composites*, 27(5), pp.507-522.
43. Niu, H. and Wu, Z., 2005. Numerical Analysis of Debonding Mechanisms in FRP-Strengthened RC Beams. *Computer-Aided Civil and Infrastructure Engineering*, 20(5), pp.354-368.
44. Niu, H., Karbhari, V.M. and Wu, Z., 2006. Diagonal macro-crack induced debonding mechanisms in FRP rehabilitated concrete. *Composites Part B Engineering*, 37(7-8), pp.627-641.
45. Rolland, A., Argoul, P., Benzarti, K., Quiertant, M., Chataigner, S. and Khadour, A., 2020. Analytical and numerical modeling of the bond behavior between FRP reinforcing bars and concrete. *Construction and Building Materials*, 231, p.117160.
46. Sebastian, W.M., 2001. Significance of midspan debonding failure in FRP-plated concrete beams. *Journal of Structural Engineering*, 127(7), pp.792-798.
47. Teng, J. ., Zhang, J. ., and Smith, S. . (2002). “Interfacial stresses in reinforced concrete beams bonded with a soffit plate a finite element study.” *Construction and Building Materials*, Elsevier, 16(1), 1–14.
48. Teng, J.G. and Chen, J.F., 2008. Mechanics of debonding in FRP-plated RC beams. In *Structures and Granular Solids* (pp. 325-338). CRC Press.
49. Yang, Z.J., Chen, J.F. and Proverbs, D., 2003. Finite element modelling of concrete cover separation failure in FRP plated RC beams. *Construction and Building Materials*, 17(1), pp.3-13.
50. Ye, J. Q. (2001). “Interfacial shear transfer of RC beams strengthened by bonded composite plates.” *Cement and Concrete Composites*, Elsevier, 23(4–5), 411–417.
51. Zhou, Y.W., Wu, Y.F. and Yun, Y., 2010. Analytical modeling of the bond–slip relationship at FRP-concrete interfaces for adhesively-bonded joints. *Composites Part B Engineering*, 41(6), pp.423-433.

SCOPUS INDEXED CONFERENCES

1. Bende, S., Kaur, N., Kumar, P., and Pal, S. (2024), “Numerical parametric study of Interfacial shear stress between Concrete and Fiber-Reinforced Polymer (FRP) on an inclined plane” 1st International Conference on Recent Advances in Infrastructure Development (RAID-2024), Department of Civil Engineering, NIT Calicut, 12th-13th February 2024.



NIT Calicut RAID 24 Brochure

Organised by



National Institute of Technology Calicut
Department of Civil Engineering

तमसो मा ज्योतिर्गमय



First International Conference
RAID24
Recent Advances in Infrastructure
Development 2024

12th and 13th FEBRUARY **2024**

In Collaboration with



RECENT DEVELOPMENTS IN STRUCTURAL, GEOTECHNICAL AND TRANSPORTATION ENGINEERING

PUBLICATION OPPORTUNITIES



ScienceDirect

click here to see more



www.nitc.ac.in raid2024@nitc.ac.in <http://www.raid2024.com>

2. Bende, S., Pal, S., Kaur, N., and Kumar, P. (2024), “A comparative analytical study of influence of varying thickness of FRP on flexural capacity of RCC beams strengthened with Fiber-Reinforced Polymer (FRP)” International Conference on Civil, Environment and Construction Technology Ecological Resilient & Sustainable Development Goals Integration – Research Agenda (CECT-2024), Department of Civil Engineering, Graphic Era (Deemed to be) University, Dehradun, 17th-18th May 2024



Graphic Era
deemed to be **University**
DEHRADUN

CERTIFICATE

OF APPRECIATION

International Conference
CECT - 2024
on
Civil, Environment and Construction Technology:
Ecological Resilient & Sustainable Development Goals
Integration- Research Agenda



This is to certify that Subodh Bende has presented a paper titled A comparative analytical study of influence of varying thickness of FRP on flexural capacity of RCC beams strengthened with FRP at the International Conference on “**Civil, Environment and Construction Technology: Ecological Resilient & Sustainable Development Goals Integration- Research Agenda**” (CECT - 2024) organized by the Department of Civil Engineering, Graphic Era (Deemed to be University), Dehradun on May 17 - 18, 2024.



Dr. Deepshikha Shukla
Organizing Secretary, CECT - 2024
Dept. of Civil Engineering
Graphic Era
(Deemed to be University)



Prof. (Dr.) Amit Srivastava
Convener, CECT - 2024
Dept. of Civil Engineering
Graphic Era
(Deemed to be University)



Prof. (Dr.) Sanjeev Kumar
Convener, CECT - 2024
Dept. of Civil Engineering
Graphic Era
(Deemed to be University)



Prof. (Dr.) K. K. Gupta
Conference Chair, CECT - 2024
Head-Dept. of Civil Engineering
Graphic Era
(Deemed to be University)

In Association with















Graphic Era deemed to be university CECT 24 Brochure

DEPARTMENT OF CIVIL ENGINEERING



Dr. Madhavi Reddy, New Jalpaiguri, Central University, UPE
 Dr. Mahesh Singh Prasad, Central University
 Dr. Praveen Kumar, NRI Institute
 Dr. Praveen K. Sharma, Professor, IT Roorkee
 Dr. Praveen Singh H., GRIJUDT, Roorkee
 Dr. Rajul Ramakrishna, IT Bombay
 Dr. Richard Fry, University of Auckland, New Zealand
 Dr. Sampath Kumar, Secretary, ACEE BIR
 Dr. Saranath Murthy Pragasam, NRI Institute
 Dr. Sureshbabu Lata Univ., of Alberta, Canada
 Dr. Shanyang Cao, Tongji University, China
 Dr. Shaili Sonam, Tilmanwala, AIIT, Bangkok
 Dr. Yachan Trivedi, Chongqing University, China
 Dr. Zhenqiang Alimad, Professor, IT Roorkee

Keynote Speakers
 Dr. Ashwajit Gupta, Director, Sheldon, Noida
 Dr. Dipankar Choudhury, Prof & Head, CED, IT Mumbai
 Dr. Dileep Singh, Prof., Texas Tech University, USA
 Dr. Kishore K. Mishra, Prof., University of Illinois, Chicago, USA
 Dr. Krishna K. Reddy, Prof., University of Illinois, Chicago, USA
 Prof. Madhusudan Karki, Professor, AMU, Aligarh
 Dr. Manjunath Vasara, Thapar University, Punjab
 Prof. Shanyang Cao, Tongji University, Shanghai, China
 Prof. Pradyuman Kumar, IIT Guwahati
 Dr. K. S. Dharti, Professor Emeritus, former Director, NRI Hyderabad
 Dr. V. S. Varma, Prof., Tokyo Polytechnic, Japan
 Dr. Zhenqiang Alimad, Professor, IT Roorkee

Tourist Attractions In and around Dehradun



Dehradun Temple
Regional Science Center
Attending Monastery
Sitthi Falls
Almora

Forest Research Institute

International Conference

CECT'2024

MAY 17-18 2024

Civil, Environment and Construction Technology: Ecological Resilient & Sustainable Development Goals Integration - Research Agenda

Publication partner
IOP Conference Series
Earth and Environmental Science

Graphic Era Deemed to be University DEHRADUN

MAAE AH ACCREDITED

Mode of Conference: Hybrid

In Association with
ASCE
AMERICAN SOCIETY OF CIVIL ENGINEERS
Headquarters: Reston, Virginia

Organized by
Department of Civil Engineering
Graphic Era (Deemed to be) University
Ball Road, Clement Town, Dehradun
Uttarakhand 248002

Website:
<http://www.cect24.org>
Email ID:
cect24@graec.edu.in






MAAE A+
MAAE A+ Accredited

#55
In University Category

07 NBA
Accredited College

601
Ranked amongst Top Universities of the World

100% E
Employability

UOE & AQCTE
University of Excellence and Accredited Quality Council of Technical Education

#189
QS World University Rankings 2022

Brand "Benchmark"
Brand "Benchmark" Award for Quality Education

PROFILE

SUBODH BENDE

CONTACT: +91 8410677874 | Email: subodhbende@yahoo.com

PROFILE

To work in a challenging environment, which demands constant development of fresh skills & the maximum utilization of the existing skills

EDUCATION

Mtech (Structural Engineering)	2022-2024	Delhi Technological University, New Delhi	8.44(SGPA)
Btech (Civil Engineering)	2011-2015	Quantum School of Technology, Roorkee	74.52%
Class XII	2010-2011	Guru Tegh Bahadur Public School, Saharanpur	79.60%
Class X	2008-2009	Guru Tegh Bahadur Public School, Saharanpur	76.00%

INTERNSHIP

Site Intern, Public Working Department, Saharanpur Division

- Participate in six week training in **PWD(2014)**, for the Construction of road under **CRF** Scheme in Saharanpur
- Gaining a knowledge of different *Estimation Techniques*.
- Gaining an Experience of *Modus Operandi* of Executive Engineer Head office

ACADEMIC PROJECTS

- Analysis and Design of “**3 Storey Office Building**”
- Project on development of “**Novel method for finding the Interfacial Shear Stress between FRP & Concrete Interface**”
- Present a Seminar on “**Effect of Magnetic water on the Engineering properties of Concrete**”
- Project Exhibition on “**Working of Rubber dam**”

WORKING EXPERIENCE

- Worked as a **Site and Billing Engineer** in *Classic Constructions* for various school, college projects from January 2016 to March 2020.
- Worked as an **Assistant Professor** in Quantum School of Technology from August 2020 to May 2022.

SOFTWARE KNOWLEDGE

- ANSYS
- STAAD.PRO
- AUTO CAD
- MS OFFICE

SKILLS & ACHIEVEMENTS

- Clear **GATE** Exam @ 4 times.
- Winner in Popsicle Sticks **Truss Bridge Design** Challenge
- Winner in Project Exhibition of **Rubber Dam**
- Acquire a 80.6 Percentile in **NCAT** Exam
- Runner up in Presentation on “**Recycling of Waste Water**”
- Runner up in **Dance Verses Poetry**, Interdepartmental Competition
- Participate in **Robotic Workshop** in **EDGE TECHFEST**

DECLARATION

I hereby declare that all the information provided in my resume is true to the best of my knowledge and belief.

PLAGIARISM REPORT